AD/A-002 879

DOPPLER VELOCITY SENSOR APN-200 ERROR MODEL AND FLIGHT TEST RESULTS

William S. Widnall, et al

Intermetrics, Incorporated

Prepared for:

Air Force Special Weapons Center

8 March 1974

Unclassified

SECURITY CLASSIFICATION OF THIS PAGE (When Data Entered)

REPORT DOCUMENTATION PAGE		READ INSTRUCTIONS BEFORE COMPLETING FORM
1. REPORT NUMBER AFSWC-TR-74-9	2. GOVT ACCESSION NO.	3. RECIPIENT'S CATALOG NUMBER AD/A-002879
4. TITLE (and Subtitle) DOPPLER VELOCITY SENSOR APN-200 ERROR MODEL AND FLIGHT TEST RESULTS		5. TYPE OF REPORT & PERIOD COVERED Contract Technical Report 6. PERFORMING ORG. REPORT NUMBER IR-78-74
7. AUTHOR(s) William S. Widnall and Peter A Grundy		8. CONTRACT OR GRANT NUMBER(s) F29601-73-C-0089
9. PERFORMING ORGANIZATION NAME AND ADDRESS Intermetrics, Inc. 701 Concord Avenue Cambridge, Mass. 02138		10. PROGRAM ELEMENT, PROJECT, TASK AREA & WORK UNIT NUMBERS 688G
11. CONTROLLING OFFICE NAME AND ADDRESS Air Force Special Weapons Center (PMRC) Kirtland Air Force Base, New Mexico 87115		12. REPORT DATE 8 March 1974 13. NUMBER OF PAGES 98
14. MONITORING AGENCY NAME & ADDRESS (if different from Controlling Office) 6585th Test Group Air Force Special Weapons Center Holloman Air Force Base, New Mexico 88330		15. SECURITY CLASS. (of this report) Unclassified 15a. DECLASSIFICATION/DOWNGRADING SCHEDULE

16. DISTRIBUTION STATEMENT (of this Report)

Approved for public release; distribution unlimited.

17. DISTRIBUTION STATEMENT (of the abstract entered in Block 20, if different from Report)

Same as above

18. SUPPLEMENTARY NOTES

19. KEY WORDS (Continue on reverse side if necessary and identify by block number)

Doppler Velocity Sensor
Teledyne-Ryan APN-200
Doppler Error Model
Doppler Flight Test Results

20. ABSTRACT (Continue on reverse side if necessary and identify by block number)

The individual sources of error in a Teledyne-Ryan APN-200 Doppler velocity measurement are discussed. Also included is the velocity error due to INS attitude reference error. A complete Doppler error model is constructed, including estimates of the one-sigma values of error parameters. Error model simplification for Kalman filter synthesis is discussed. Data, from a 7 August 1973 flight test of an APN-200 at Holloman Air (over)

DD FORM 1 JAN 73 1473 EDITION OF 1 NOV 65 IS OBSOLETE

Unclassified

SECURITY CLASSIFICATION OF THIS PAGE (When Data Entered)

Block 20

Force Base, are analyzed. The Doppler velocity performance, including random noise level and slowly varying error, is found to be in agreement with the accuracy predicted by the error model.

FOREWORD

This technical report has been prepared by Intermetrics for the 6585th Test Group, Holloman Air Force Base, New Mexico, under Contract F29601-73-C-0089. The technical monitor of this contract has been Capt. Walter G. Murch.

The discussions of Doppler sensor principles and functional design (Chapter 2), sources of Doppler velocity error (Chapter 3), and the summary and conclusions (Chapter 5) were written by Dr. William S. Widnall. Statistical analysis of the Doppler flight test data was performed by Mr. Peter A. Grundy, who also summarized the results (Chapter 4). The manuscript has been prepared by Ruth Lepson and Eileen Martin.

ABSTRACT

The individual sources of error in a Teledyne-Ryan APN-200 Doppler velocity measurement are discussed. Also included is the velocity error due to INS attitude reference error. A complete Doppler error model is constructed, including estimates of the one-sigma values of error parameters. Error model simplification for Kalman filter synthesis is discussed. Data, from a 7 August 1973 flight test of an APN-200 at Holloman Air Force Base, are analyzed. The Doppler velocity performance, including random noise level and slowly varying error, is found to be in agreement with the accuracy predicted by the error model.

CONTENTS

ILLUSTRATIONS

TABLES

CHAPTER 1

INTRODUCTION

The CIRIS (Completely Integrated Reference Instrumentation System) has been developed by Holloman Air Force Base to provide a highly accurate aircraft navigation reference for the test and evaluation of advanced guidance and navigation systems. The CIRIS flight hardware as originally implemented includes a Litton CAINS inertial navigator with barometric altimeter, a Cubic Corp. CR-100 precision range/range-rate measurement system, and a Hewlett Packard 2100 general purpose digital computer. Intermetrics has provided a Post-Flight Processor (PFP) -- a system of computer programs -- for the optimal estimation of aircraft position, velocity, and attitude from the flight-recorded inertial and precision-ranging data. The forward-filtering portion of the PFP (the Kalman filter) has been transferred to the onboard computer to provide in-flight real-time accurate indications of the aircraft navigation state.

Recently a Teledyne-Ryan APN-200 Doppler velocity sensor has been procured and has been added to the CIRIS flight hardware. Intermetrics has been asked to modify the CIRIS Post-Flight Processor to incorporate the Doppler measurements into the optimal estimation of aircraft navigation state. A first step that is required is the selection or development of a statistical error model representing the sources of velocity error in the APN-200 Doppler velocity sensor. This report summarizes this first step.

Chapter 2 discusses general Doppler sensor principles plus the specific functional design of the APN-200. The single-beam Doppler shift and then the measurement of vector velocity using multiple beams are discussed. A brief functional description of the APN-200 provides necessary background for the discussion of sources of error. Performance limits that are implied by the functional design are discussed.

Chapter 3 discusses the individual sources of error in a Doppler velocity measurement. Many of the sources of error are a function of the design of the Doppler velocity sensor. In addition, several external environment factors are sources of error. Also included in the error discussion is the velocity error due to attitude reference error. The emphasis is placed on identifying the physical parameters which cause the velocity errors. With this physical understanding, one can construct a Doppler error model which exhibits the correct dependence on flight variables such as speed and attitude. Also the number of error parameters to be determined from flight test data can be held to a minimum.

Chapter 4 summarizes statistical analyses of the velocity data from a flight test of the APN-200 out of Holloman AFB, using the other CIRIS subsystems to estimate the true aircraft velocity. The estimated errors of the CIRIS reference velocity are presented. The flight is divided into several segments for individual analysis. The measured differences between the Doppler velocity and the CIRIS reference velocity are analyzed with respect to velocity random error and velocity slowly varying error. The measured statistics are compared with the Doppler error model of Chapter 3.

Chapter 5 presents a summary and the conclusions.

CHAPTER 2

DOPPLER SENSOR PRINCIPLES AND FUNCTIONAL DESIGN

2.1 Single Beam Doppler Shift

A Doppler velocity sensor may radiate one or more beams of electromagnetic energy toward the surface of the earth. Some of the energy illuminating the surface is scattered back toward the Doppler sensor. If there is relative motion between the Doppler antenna and scatterers on the surface, then the energy returned is shifted in frequency. This is called the Doppler shift. The Doppler frequency shift for a given beam is

$$f = \frac{2}{\lambda} v \cos\alpha \qquad (2\text{-}1)$$

where λ is the wavelength of the carrier-frequency radiation, v is the magnitude of the aircraft velocity vector relative to the surface, and α is the angle between the antenna beam and the velocity vector. The frequency is shifted on transmission and again on reception, which accounts for the factor of two in Equation 2-1.

The constant $2/\lambda$ is called the Doppler sensitivity s to the aircraft velocity component along the beam axis. In terms of the speed of light c and the carrier frequency f_c, the sensitivity may also be expressed as

$$s = 2/\lambda = 2f_c/c \qquad (2\text{-}2)$$

For the APN-200 with a transmission frequency of 13.3 GHz, the Doppler sensitivity is 45.6 Hz/knot.

2.2 Measurement of Vector Velocity

By measuring the Doppler shift along three or more non-coplanar directions, one can calculate the three orthogonal components of aircraft velocity. The APN-200 generates four beams at fixed orientations with respect to the aircraft, as illustrated in Figure 2-1, from Reference [1]. The figure also shows an aircraft-referenced orthogonal coordinate system. The subscripts h, d, and z denote the along-heading, cross-heading (or drift), and down components respectively. Positive directions are forward, right, and down. In terms of the three orthogonal components of aircraft velocity, the Doppler shift along a beam is

$$f = s(v_h \cos\nu_h + v_d \cos\nu_d + v_z \cos\nu_z) \qquad (2\text{-}3)$$

where ν_h, ν_d, ν_z are the angles between the coordinate axes and beam axis.

The beam orientations in the APN-200 have fore-and-aft and lateral symmetry. Hence the direction cosines for all beams are the same, except for sign. The nominal Doppler shifts are

$$\begin{aligned} f_1 &= s(+\ell\, v_h - m\, v_d + n\, v_z) \\ f_2 &= s(-\ell\, v_h - m\, v_d + n\, v_z) \\ f_3 &= s(-\ell\, v_h + m\, v_d + n\, v_z) \\ f_4 &= s(+\ell\, v_h + m\, v_d + n\, v_z) \end{aligned} \qquad (2\text{-}4)$$

where ℓ, m, n are the magnitudes of the beam direction cosines. It is clear that the desired aircraft-referenced velocity components can be computed as a function of the four Doppler shifts as

$$\begin{aligned} v_h &= \frac{1}{4s\ell}(+ f_1 - f_2 - f_3 + f_4) \\ v_d &= \frac{1}{4sm}(- f_1 - f_2 + f_3 + f_4) \\ v_z &= \frac{1}{4sn}(+ f_1 + f_2 + f_3 + f_4) \end{aligned} \qquad (2\text{-}5)$$

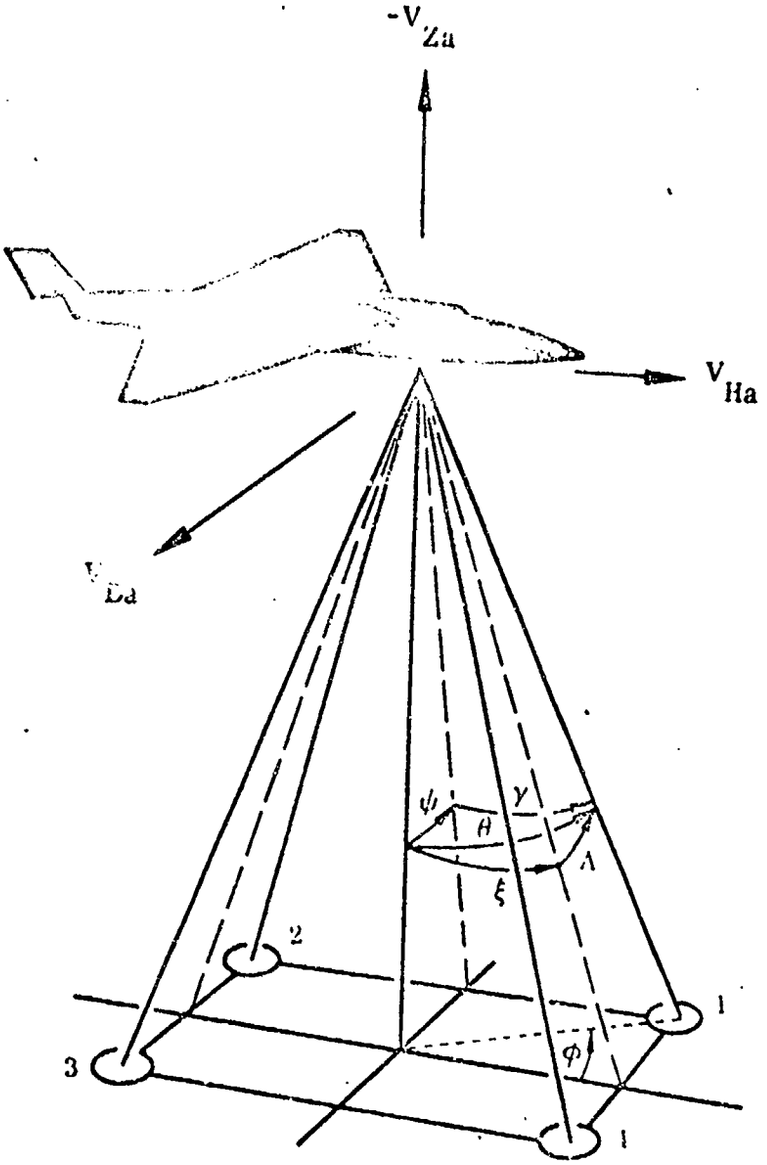

Fig. 2-1 Four-Beam Doppler Geometry[1]

Alternate solutions for the velocity components are

$$v_h = \frac{1}{2s\ell}(+ f_1 - f_2) \text{ or } \frac{1}{2s\ell}(- f_3 + f_4)$$

$$v_d = \frac{1}{2sm}(- f_2 + f_3) \text{ or } \frac{1}{2sm}(- f_1 + f_4) \qquad (2\text{-}6)$$

$$v_z = \frac{1}{2sn}(+ f_1 + f_3) \text{ or } \frac{1}{2sn}(+ f_2 + f_4)$$

The APN-200 mechanizes the four-beam solution (Equation 2-5) when all four Doppler beams are usable. If one beam becomes unusable, the system automatically switches to the appropriate three-beam solution from Equation 2-6. When all four beams seem usable, the redundant information provides a consistency test, because in theory from Equation 2-4

$$f_1 - f_2 + f_3 - f_4 = 0 \qquad (2\text{-}7)$$

For the angles defined in Figure 2-1, the direction cosines are

$$\begin{aligned} \ell &= \sin\gamma = \sin\theta\cos\phi = \cos\Lambda\sin\xi \\ m &= \cos\gamma\sin\psi = \sin\theta\sin\phi = \sin\Lambda \\ n &= \cos\gamma\cos\psi = \cos\theta = \cos\Lambda\cos\xi \end{aligned} \qquad (2\text{-}8)$$

The nominal beam angles of the APN-200 are

$$\begin{aligned} \gamma &= 20^\circ\ 26' & \xi &= 20^\circ\ 53' \\ \psi &= 12^\circ\ 23' & \Lambda &= 11^\circ\ 35' \\ \theta &= 23^\circ\ 46' & \phi &= 29^\circ\ 54' \end{aligned} \qquad (2\text{-}9)$$

for which the nominal values of the direction cosines are

$$\begin{aligned} \ell &= .349 \\ m &= .201 \\ n &= .915 \end{aligned} \qquad (2\text{-}10)$$

2.3 APN-200 Functional Description

A block diagram of the APN-200 Doppler velocity sensor is presented in Figure 2-2, from Reference [1].

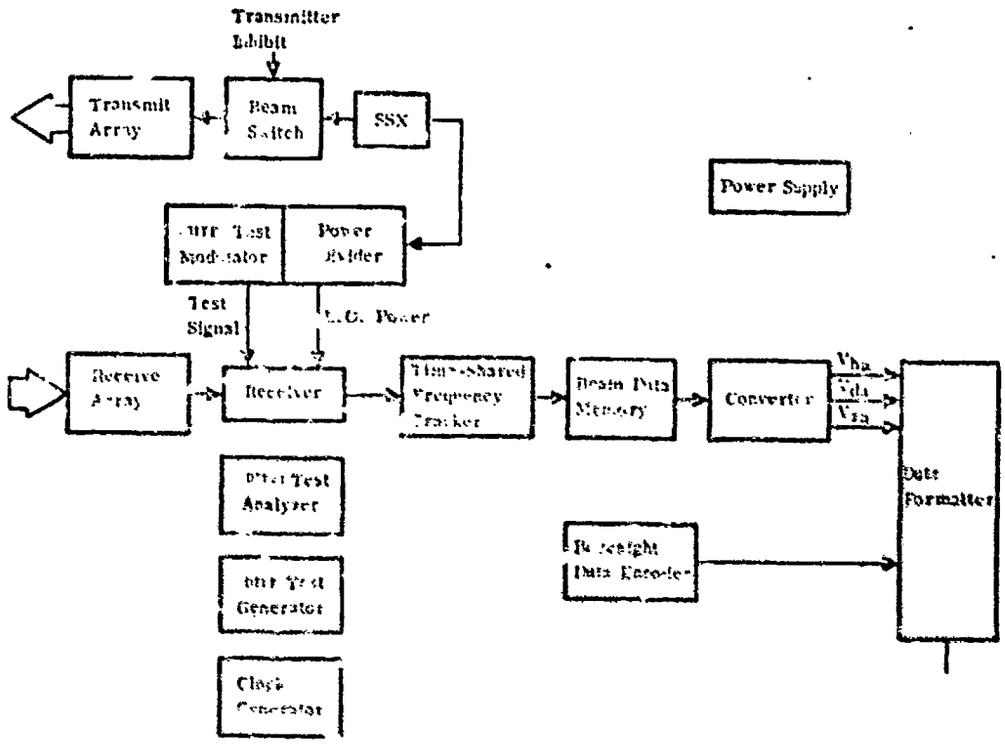

Figure 2-2

Block Diagram of APN-200 Doppler Velocity Sensor[1]

Doppler-frequency measurements are obtained sequentially (not simultaneously) for each of the four beam directions. There are two antenna arrays, one for transmitting and one for receiving. The transmitter array has two ports. When port 1 is energized by the transmitter, energy is radiated along the diagonally-opposite beams 1 and 3. When port 2 is energized the transmitter energy is radiated along the other diagonal beam-pair 2 and 4. The receiver array also has two ports. The energy received from the two forward beam directions is channeled to one port. The energy received from the two aft beam direction is channeled to the other port. A solid state switch is used to switch the transmitter between transmit-array input ports 1 and 2. Similarly, a switch, at the Doppler-frequency-tracker input, alternates between the outputs of the receivers at port 1 and 2 of the receive array. The four possible combinations of the two transmit-switch states and the two receive-switch states produces the four separately-selectable directions for Doppler measurements. The switches are cycled such that 62.5 msec is devoted to the measurement at each direction. The sequence of four measurements takes 0.25 sec. A consequence of this design is that three of the Doppler shifts used to compute current velocity are old, introducing a small lag into the indicated current velocity.

The receiving antenna array is configured to form pairs of lobes for each beam. Through the use of microwave hybrid mixers, the phase sums and differences of the pairs of lobes are provided for data processing. The sum of a pair of lobes is a pencil beam with beamwidths somewhat greater than a single lobe. The difference of a pair of lobes generates a uniquely defined null beam axis. This null axis is determined solely by array geometry; it is not influenced by terrain reflectivity. By tracking the null, Teledyne Ryan indicates terrain bias is substantially eliminated from the measured forward component of velocity[1].

Energy received from each radar beam is detected by heterodyning it with a portion of the transmitted signal (zero-frequency super heterodyne detection) and is amplified. A portion of the energy received from the sum radar beam is detected as a reference Doppler signal in one mixer detector. The remainder is detected in phase quadrature with the reference signal in a second mixer.

The Doppler spectra from the receivers are acquired and tracked in the frequency tracker. Only one frequency tracker is utilized. It is sequentially switched to the appropriate receiver. Teledyne Ryan states that this single channel design saves space, weight, and power, and increases reliability[1]. For each beam, the frequency tracker searches the band of expected Doppler frequencies, acquires the Doppler signal, and tracks the center-of-power of the spectrum. The energy received from the difference arm of the microwave hybrid is detected in a third mixer. The Doppler data from the difference channel is cross-correlated with data from the sum channel by the difference tracker to produce a signal frequency in a digital frequency synthesizer corresponding to the beam null Doppler frequency.

Each beam Doppler signal is independent and is present in the tracker one-fourth of the time. At the end of each beam time-shared period, information pertaining to that beam is stored in tracker memory to be recalled when the respective beam signal command appears. This makes acquisition independent for each signal.

The time-shared tracker produces output serial binary statements of velocity along each of the four beams. The converter performs serial binary arithmetic to compute the orthogonal velocity components in aircraft coordinates. The converter transmits the velocity data to the user (usually a general purpose digital computer) in the form of word-serial bit-serial binary numbers.

Antenna boresight calibration data are determined at the factory and are encoded in a read-only memory for transmission to the user upon interrogation. The calibration data are applied by the user to the uncorrected sensor velocity outputs.

2.4 Performance Limits

The four beams are clustered near straight down so that the aircraft may roll and pitch through substantial angles without loss of any beam return signal. It is clear that no return signal will be detected if a beam is above horizontal. For the APN-200 angles (Equation 2-9) the roll attitude and pitch attitude that cause horizontal beams are roll ± 78° (at zero pitch) and pitch ± 69° (at zero roll). The actual

attitude limits are smaller than these absolute limits because the return signal becomes too weak for detection well before a beam reaches horizontal. The attitude at which signal is too weak is a function of transmitter power, antenna gain, the terrain backscattering coefficient, the angle of incidence, the altitude above the terrain, and the receiver noise. The APN-200 is specified as functioning through ± 45° in roll and ± 25° in pitch at 40,000 feet altitude. At a lower altitude of 5,000 feet the limits increase to ± 60° in roll and ± 30° in pitch. The above limits are for a worst case surface, which is smooth water (Beauford-one sea state). For rough water or land, larger attitude excursions should be possible without loss of signal.

A consequence of clustering the beams near straight down is the reduction in Doppler sensitivity to forward and lateral velocities. The Doppler sensitivities for the APN-200 to forward, lateral, and vertical velocities are

$$s_h = s\ell = 15.9 \text{ Hz/knot}$$

$$s_d = sm = 9.2 \text{ Hz/knot} \qquad (2\text{-}11)$$

$$s_z = sn = 41.8 \text{ Hz/knot}$$

The Doppler frequency tracker in the APN-200 does not have a zero frequency offset. Therefore the tracker is unable to distinguish between positive Doppler frequency (positive velocity along the beam) and negative Doppler frequency (negative velocity along the beam). The APN-200 sensor is intended for aircraft applications where the velocity vector is generally in the forward direction. The mechanization therefore can assume that the forward beam Doppler shift frequencies (f_1 and f_4) are positive and the aft beam Doppler shift frequencies (f_2 and f_3) are negative. The appropriate sets of mechanization equations (where all measured Doppler frequencies are positive numbers) are obtained by reversing the signs of the aft-beam frequencies f_2 and f_3 in Equations 2-5, 2-6, and 2-7.

This mechanization is not appropriate for a helicopter, which can fly backwards, sideways, or straight up and down. In each of these cases, assuming the tracker finds the Doppler signals, this mechanization would give an incorrect velocity indication because either a forward beam is receiving a negative Doppler shift or an aft beam is receiving a positive Doppler shift.

The frequency tracker has a high-pass filter at the input to reject noise below 500 Hz. As a result, the tracker will not find Doppler frequencies below about 500 Hz. The Doppler frequency along each beam is of the form

$$f = s_h v_h \pm s_d v_d \pm s_z v_z \qquad (2\text{-}12)$$

For the APN-200 sensitivities given in Equation 2-11 and because the Doppler frequency must be above 500 Hz, the vehicle velocity components must satisfy

$$15.9 v_h \pm 9.2 v_d \pm 41.8 v_z > 500 \text{ Hz} \qquad (2\text{-}13)$$

where the velocity components are expressed in knots. At zero drift and vertical velocity, a minimum speed of about 30 knots is required for the Doppler to function. Thus no Doppler data are available at rest or at slow taxi speeds.

Drift velocity limits also can be inferred from Equation 2-13. The worst case is at slow speeds and high angles of attack. For example, if an aircraft has heading velocity of 100 knots and vertical velocity of 13 knots, then drift velocity cannot exceed 60 knots. This is a drift angle limit of about 30°.

CHAPTER 3

DOPPLER ERROR MODEL

3.1 Introduction

This chapter discusses the various sources of velocity error in a Doppler velocity measurement. Of interest are not only those sources of error inherent in the electronics and functional design of the Doppler velocity sensor, but also the sources of error in the external environment. Furthermore, to be useful for navigation, the aircraft-referenced measurement velocity components must be transformed to navigation-frame coordinates (such as an east-north-up set). Thus in addition to the Doppler equipment and environment errors, there are velocity errors due to attitude-reference errors.

If optimal filtering is to be used to mix the Doppler-velocity-measurement data with inertial or other navigation data, then for filter synthesis the designer requires estimates of the statistics of the Doppler-velocity-measurement errors. Statistical parameters of interest include: RMS level of the uncorrelated random error (noise) in each velocity component, cross-correlation between component errors, uncompensated bias magnitudes, and slowly-varying error RMS levels and correlation times.

The emphasis in this chapter is placed on identifying the physical parameters which cause the velocity errors. With this physical understanding, one can construct an error model which exhibits the correct dependence on flight variables, such as speed and attitude. Also the number of error parameters to be determined from flight test data can be held to a minimum.

Typical values for the sources of error are mentioned, including estimates of values for the APN-200 by Teledyne Ryan. Measured parameter values from flight test data are presented in Chapter 4.

3.2 Noise Due to Finite Beamwidth

3.2.1 Doppler Bandwidth and Correlation Time

The indicated velocity from a Doppler velocity sensor is very noisy. This is related to the finite width of each Doppler beam, one of which is shown in Figure 3-1. The single Doppler frequency of an infinitely narrow beam was given in Equation 2-1. But with a finite beamwidth, the Doppler spectrum is broadened. Energy returned by scatterers at the forward edge of the beam will have a higher Doppler frequency than that of the energy returned by scatterers at the aft edge of the beam. The bandwidth Δf of the Doppler signal is given approximately by the differential (with respect to look-angle α) of Equation 2-1

$$f = s\, v \cos\alpha \qquad (2\text{-}1)$$

repeated (3-...

$$\Delta f = s\, v\, \Delta\alpha \sin\alpha$$

where s is the Doppler sensitivity $2/\lambda$ and $\Delta\alpha$ is the beamwidth (in the plane of the velocity vector and the nominal beam direction).

An alternate expression which shows the dependence of Doppler bandwidth upon the shape of the beam is [3]

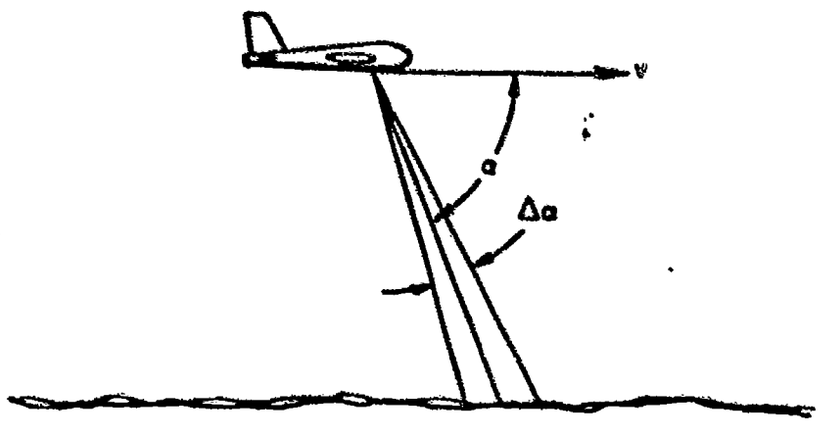

Figure 3-1

Finite Doppler Beam Width

$$\Delta f = s[v_1^2 \beta^2 + v_2^2 \eta^2 + \frac{1}{16\ell n2} v_3^2 (\beta^4 + \eta^4)]^{1/2} \quad (3\text{-}2)$$

where

Δf = Doppler signal 3db bandwidth

s = Doppler sensitivity $2/\lambda$

v_1, v_2, v_3 = velocity components in beam coordinates

β, η = minor and major two-way 3db radian beamwidths

For the APN-200, the two-way minor-axis beamwidth (fore-and-aft direction) is 1.8° (.032 radian) and the major-axis beamwidth (lateral direction) is 3.4° (.06 radian)[1]. For small to moderate drift angles, the largest term in Equation 3-2 would be the forward-velocity-minor-axis term.

The relative (fractional) spectrum width is frequently of interest, and is found by dividing Equation 3-1 by Equation 2-1.

$$\frac{\Delta f}{f} = \Delta\alpha \tan \alpha \quad (3\text{-}3)$$

For a .032 radian beamwidth and a look angle of 70° (APN-200 with zero drift and vertical velocity) the relative spectrum width is 9 percent. Other Doppler radars having wider beams have relative spectrum widths of 15 to 25 percent[2].

The period of time during which the frequency and phase of the signal are approximately constant is called the Doppler correlation time. The correlation time τ_f is proportional to the reciprocal of the spectrum half width $\Delta\omega/2$[4]

$$\tau_f = 2/\Delta\omega = 1/(\pi\Delta f) \quad (3\text{-}4)$$

Note from Equation 3-1 that the Doppler bandwidth is directly proportional to vehicle velocity, and therefore the Doppler correlation time is inversely proportional to velocity. For the APN-200 with .032 radian beamwidth, look angle of 70°, sensitivity of 45.6 Hz/knot, and assuming an aircraft speed of 400 knots, the Doppler bandwidth from Equation 3-1 is 550 Hz. The Doppler correlation time from Equation 3-4 is .0006 sec. Fried[2] points out the interesting fact that the Doppler correlation time is of the order of the time required for the vehicle to travel a distance equal to the length of the antenna.

3.2.2 Variance of Single-Beam Velocity Error

If the Doppler frequency tracker could follow the rapid fluctuations of the instantaneous frequency random process, then the measured velocity along the beam would exhibit very large velocity random error. The one-sigma deviation of the instantaneous frequency random process from its mean value is approximately half the Doppler signal bandwidth[4].

$$\sigma_f = \Delta f/2 \tag{3-5}$$

For the 400 knot example, for which the Doppler bandwidth is 550 Hz, the one-sigma frequency deviation is 225 Hz. For the Doppler sensitivity of 45.6 Hz/knot, this is a one-sigma beam velocity error of 6 knots.

To reduce the amplitude of the random velocity error it is desireable to filter the noise. A practical frequency tracker has an output time constant τ_v that is greater than the correlation time τ_f of the Doppler signal. The APN-200 has output correlation of about .2 sec. Therefore the frequency measurement error out of the tracker has variance reduced to

$$\sigma_f'^2 = \sigma_f^2 \, \tau_f/\tau_v \tag{3-6}$$

Measured velocity is related to measured Doppler frequency by the Doppler sensitivity factor s. The error in measured velocity is similarly related to the error in measured frequency

$$\sigma_v = \sigma_f'/s \tag{3-7}$$

The velocity error of the APN-200 will be somewhat noisier than implied by the above equations. This is because systems employing lobing techniques (for terrain bias error suppression) have random error variance increased by a factor[2]

$$\beta = \Delta f/W_f \tag{3-8}$$

where Δf is the Doppler signal bandwidth and W_f is the lobing low-pass tracker-filter bandwidth. This filer bandwidth is an intermediate bandwidth, not the same as the narrow bandwidth associated with the output correlation time τ_v. The tracker bandwidth of the APN-200 is adjusted in steps as a function of the measured Doppler frequency. At 400 knots, the single beam Doppler frequency is about 6400 Hz. This is in the middle of the 4000 to 8000 Hz range for which the tracker bandwidth is set at 60 Hz. The Doppler bandwidth at 400 knots was noted to be 550 Hz, so the variance increase factor (Equation 3-8) is about 10.

Combining the above relationships, the variance of single-beam velocity measurement error is

$$r_b = \sigma_v^2 = \frac{v\ \beta\ \Delta\alpha\ \sin\alpha}{4\ \pi\ s\ \tau_v} \tag{3-9}$$

where

v = magnitude of vehicle velocity

β = mechanization variance-increase factor

$\Delta\alpha$ = beamwidth

α = angle between velocity vector and beam

s = Doppler sensitivity

τ_v = output time constant

Note the velocity error variance is proportional to velocity (assuming that the step changes in tracker bandwidth keep β (Equation 8) approximately constant). For $\beta = 10$, $\Delta\alpha = .032$ radian, $\alpha = 70°$, $s = 45.6$ Hz/knot, and $\tau_v = .2$ sec, the APN-200 should have single-beam velocity error variance of about .0026 knots^2/knot. At 400 knots this would be 1.0 knots^2 or (1.0 knot)^2.

The variance of the random error could be reduced by lengthening the output time constant. However, this would increase the lag error, which occurs when velocity along a beam is changing.

3.2.3 Three-Axis Covariance of Velocity Errors

The velocity random error of each beam is uncorrelated with the errors of the other beams, because an independent set of scatterers is providing the Doppler return for each beam. Assuming small drift and vertical velocity, the four-beam array symmetry implies equal velocity-error variance for each beam.

The velocity errors δv_h, δv_d, δv_z in the aircraft-referenced velocity components, for the four-beam mechanization of Equation 2-5, are

$$\delta v_h = \frac{1}{4\ell} (+\delta v_1 - \delta v_2 - \delta v_3 + \delta v_4)$$

$$\delta v_d = \frac{1}{4m} (-\delta v_1 - \delta v_2 + \delta v_3 + \delta v_4) \qquad (3\text{-}10)$$

$$\delta v_z = \frac{1}{4n} (+\delta v_1 + \delta v_2 + \delta v_3 + \delta v_4)$$

where δv_1, δv_2, δv_3, δv_4 are the velocity errors of the four beams and ℓ, m, n are the beam direction cosines. If the individual beam errors have zero mean, then the component errors also have zero mean. It can be shown, using the assumed zero correlation between beam errors, that the variances r_h, r_d, r_z of the component velocity errors are

$$r_h = r_b/(4\ell^2)$$

$$r_d = r_b/(4m^2) \qquad (3\text{-}11)$$

$$r_z = r_b/(4n^2)$$

where r_b is the single-beam velocity error variance (Equation 3-9). For the APN-200 direction cosines of .349, .201, .915 the component variances are

$$r_h = 2.1\ r_b$$

$$r_d = 6.2\ r_b \qquad (3\text{-}12)$$

$$r_z = 0.3\ r_b$$

One might expect the cross-correlation between component velocity errors to be non-zero, because the error of each beam contributes to the error of all three components. However it can be shown (by computing the expectation of the product of pairs of equations in set 3-10) that the cross-correlation is zero. This result is due to the four-beam symmetry whereby positive correlation due to one beam error is offset by equal but negative correlation due to another beam error. Thus the covariance matrix of the aircraft-coordinate velocity vector noise error is theoretically

$$R = r_b \begin{bmatrix} 2.1 & 0 & 0 \\ 0 & 6.2 & 0 \\ 0 & 0 & 0.3 \end{bmatrix} \qquad (3\text{-}13)$$

If the single-beam variance is about .0026 knot^2/knot, as discussed earlier, the covariance should be about

$$R = v \begin{bmatrix} .0055 & 0 & 0 \\ 0 & .0161 & 0 \\ 0 & 0 & .0008 \end{bmatrix} \qquad (3\text{-}14)$$

where v is in knots to obtain velocity error variance R in knots^2.

The above variance values, obtained from theoretical considerations, may be compared with the noise specifications for the APN-200. The noise specifications are that the output noise spectral densities P_h, P_d, P_z shall be less than .001, .002, .0005 knot^2/(radian/sec)/knot[1]. These are one-sided power spectral densities in angular frequency that are related to velocity error variance by[2]

$$r = v\ P\ \pi/\tau_v \qquad (3\text{-}15)$$

For the output time constant or correlation time τ_v of .2 sec, the specified error covariance matrix is

$$R = v \begin{bmatrix} .016 & 0 & 0 \\ 0 & .031 & 0 \\ 0 & 0 & .008 \end{bmatrix} \qquad (3\text{-}16)$$

The estimated component variances (Equation 3-14) are seen to be smaller than the specification (Equation 3-16).

3.2.4 Significance of Doppler Noise Error

It is interesting to note that the position error due to the velocity noise is a function of distance traveled but is not a function of speed. Consider a Doppler navigator that computes position by integrating velocity in a digital computer. Assuming the computer samples velocity every Δt sec, the position error due to velocity error at the end of n sample intervals is

$$\delta p = \sum_{i=1}^{n} \delta v_i \, \Delta t \qquad (3\text{-}17)$$

Assuming uncorrelated random velocity error (Δt greater than the error correlation time), the variance of the position error is

$$r_{\delta p} = n \, r_{\delta v} \, \Delta t^2 \qquad (3\text{-}18)$$

But the velocity error variance is proportional to velocity, as indicated in Equation 3-14. Hence the position error variance is of the form

$$r_{\delta p} = n \, v \, k \, \Delta t^2 \qquad (3\text{-}19)$$

The distance traveled is

$$d = n \, v \, \Delta t \qquad (3\text{-}20)$$

So, Equation 3-19 also may be written

$$r_{\delta p} = d \, k \, \Delta t \qquad (3\text{-}21)$$

which shows that the position error variance due to the velocity noise is not a function of speed.

The noisy nature of the output of a Doppler velocity sensor may be bothersome in applications where the instantaneous indicated velocity must be very accurate. However in Doppler navigation, where position error is of greatest interest, the effect of the random noise velocity error is reduced to a negligible level compared with other sources of error after only a few miles distance traveled. The fractional one-sigma position error due to velocity noise is from Equation 3-21

$$\sigma_{\delta p}/d = (k \, \Delta t/d)^{1/2} \qquad (3\text{-}22)$$

Assuming a velocity error variance factor k at the specified level of .016 knots^2/knot, sample interval Δt of 1.0 sec (1/3600 hr), and distance traveled d of 10 naut. mi, then the fractional one-sigma position error is .0007 of distance traveled. This is smaller than the error due to a typical bias velocity error, which is of the order .001 of distance traveled.

3.3 Tracker Time Constant

The Doppler frequency tracker in the APN-200 has a time constant of about 0.2 sec. By having a noticeable time constant, the tracker filters the very large velocity-error noise inherent in the Doppler signal. However by having a noticeable time constant, a lag error is introduced whenever velocity along a beam changes.

In addition to the lag due to the frequency tracker time constant, there is in the APN-200 a lag due to the single-channel four-beam sampling mechanization. The effective time constant due to both the tracker time constant and the sample-and-hold mechanization is about 0.25 sec.

The lag error can be noticeable during speed changes. Consider that the aircraft accelerates from 300 to 420 knots in 60 sec (about 0.2g acceleration). The tracker time constant of 0.25 sec will cause a 0.5 knot velocity error, which will persist during the 60 sec period.

In the absence of wind, the aircraft can maneuver at constant speed without incurring a Doppler lag error. This is because an aircraft normally flies at small angle-of-attack and sideslip angle whether straight and level, or in a coordinated turn, or climbing, or descending. The ground speed vector has nearly constant components in aircraft-fixed directions and in particular in the beam directions.

However if there is a strong wind aloft, the ground speed vector may not be aligned with the longitudinal axis of the aircraft. In this case roll rate or heading rate causes a velocity lag error. Consider a cross wind of 100 knots and a roll rate of 10 deg/sec (1/6 rad/sec). The tracker time constant of 0.25 sec will cause a 4 knot velocity error for the

few seconds that the aircraft is rolling at that rate. Initially, at zero roll angle the velocity error is substantially in the v_z "vertical" component. At steep roll angles, the error due to roll rate is also seen in the v_d "drift" component.

In a shallow turn at a heading rate of 3 deg/sec (1/20 rad/sec), the 100 knot wind and 0.25 sec tracker time constant cause a velocity error of 1.2 knots. When the track is across the wind, the error is mostly in the heading direction. When the track is along the wind, the error is mostly in the "drift" direction. The turn duration at 3 deg/sec for a 180 deg turn is 60 sec.

3.4 Beam Direction Errors

The center of each beam will never lie precisely along the intended nominal direction, because of three factors: 1) normal manufacturing tolerances produce an antenna having boresights slightly off of the nominal directions; 2) changes in antenna temperature change the physical size of the antenna and therefore shift the directions of the beams; 3) the antenna will not be mounted on the aircraft in precisely the intended nominal orientation. These sources of beam direction error and their effect on velocity error are discussed in this section. The terrain bias effect, which might also be considered a beam direction error, is discussed in Section 3.5.

3.4.1 Residual Errors After Compensation

The Doppler frequency shifts along each of the four nominal beam directions were given in Equation 2-4. In terms of the actual beam directions, the Doppler shifts are

$$\begin{bmatrix} f_1 \\ f_2 \\ f_3 \\ f_4 \end{bmatrix} = s \begin{bmatrix} \ell_1 & -m_1 & n_1 \\ -\ell_2 & -m_2 & n_2 \\ -\ell_3 & m_3 & n_3 \\ \ell_4 & m_4 & n_4 \end{bmatrix} \begin{bmatrix} v_h \\ v_d \\ v_z \end{bmatrix} \qquad (3\text{-}23)$$

where the ℓ_i, m_i, n_i are the magnitudes of the i-th beam direction cosines. The velocity computation (Equation 2-5) expressed in matrix form is

$$\begin{bmatrix} \hat{v}_h \\ \hat{v}_d \\ \hat{v}_z \end{bmatrix} = \frac{1}{4s} \begin{bmatrix} 1/\ell & -1/\ell & -1/\ell & 1/\ell \\ -1/m & -1/m & 1/m & 1/m \\ 1/n & 1/n & 1/n & 1/n \end{bmatrix} \begin{bmatrix} f_1 \\ f_2 \\ f_3 \\ f_4 \end{bmatrix} \qquad (3\text{-}24)$$

where $\hat{v}$ denotes the computed velocity. Note the velocity computation is based on the nominal direction cosine magnitudes ℓ, m, n. Combining Equation 3-24 and Equation 3-23, the computed velocity is related to the true velocity as

$$\begin{bmatrix} \hat{v}_h \\ \hat{v}_d \\ \hat{v}_z \end{bmatrix} = \begin{bmatrix} (\ell_1+\ell_2+\ell_3+\ell_4)/4\ell & (-m_1+m_2-m_3+m_4)/4\ell & (n_1-n_2-n_3+n_4)/4\ell \\ (-\ell_1+\ell_2-\ell_3+\ell_4)/4m & (m_1+m_2+m_3+m_4)/4m & (-n_1-n_2+n_3+n_4)/4m \\ (\ell_1-\ell_2-\ell_3+\ell_4)/4n & (-m_1-m_2+m_3+m_4)/4n & (n_1+n_2+n_3+n_4)/4n \end{bmatrix} \begin{bmatrix} v_h \\ v_d \\ v_z \end{bmatrix}$$

(3-25)

Note that if all actual direction cosines had the nominal values, the above matrix would be the identity matrix and the computed velocity would equal the true velocity. If one replaces the actual direction cosines in Equation 3-25 by the equivalent nominal value plus error ($\ell_1 \equiv \ell + \delta\ell_1$ etc.), it can be shown that the computed velocity $\underline{v}$ and the velocity error $\delta\underline{v}$ are

$$\hat{\underline{v}} = (I + E)\ \underline{v} \tag{3-26}$$

$$\delta\underline{v} = E\ \underline{v} \tag{3-27}$$

where E is the error matrix whose nine elements are

$$\begin{aligned}
E_{hh} &= (\delta\ell_1 + \delta\ell_2 + \delta\ell_3 + \delta\ell_4)/4\ell \\
E_{hd} &= (-\delta m_1 + \delta m_2 - \delta m_3 + \delta m_4)/4\ell \\
E_{hz} &= (\delta n_1 - \delta n_2 - \delta n_3 + \delta n_4)/4\ell \\
E_{dh} &= (-\delta\ell_1 + o\ell_2 - \delta\ell_3 + \delta\ell_4)/4m \\
E_{dd} &= (\delta m_1 + \delta m_2 + \delta m_3 + \delta m_4)/4m \\
E_{dz} &= (-\delta n_1 - \delta n_2 + \delta n_3 + \delta n_4)/4m \\
E_{zh} &= (\delta\ell_1 - \delta\ell_2 - \delta\ell_3 + \delta\ell_4)/4n \\
E_{zd} &= (-\delta m_1 - \delta m_2 + \delta m_3 + \delta m_4)/4n \\
E_{zz} &= (\delta n_1 + \delta n_2 + \delta n_3 + \delta n_4)/4n
\end{aligned} \tag{3-28}$$

The subscript convention in Equation 3-28 is E_{hd} is in the h row and d column, such that $\delta v_h = E_{hd}\ v_d$, etc.

Assume that the one-sigma levels of the forward and lateral boresight errors $\delta\ell$ and δm are about 2 milliradian

$$\sigma_\ell = \sigma_m = 0.002 \text{ radian} \tag{3-29}$$

The change in the third component δn is not independent because the sum of the squares of the three direction cosines must be unity. It can be shown for small errors

$$\delta n = (-\ell\ \delta\ell - m\delta m)/n \tag{3-30}$$

Assuming $\delta\ell$ and δm are statistically independent, the one sigma value of δn is

$$\sigma_n = [\ell^2\ \sigma_\ell^2 + m^2\ \sigma_m^2]^{1/2}/n \tag{3-31}$$

which for nominal beam direction cosines ℓ, m, n of .349, .201, .915 and $\sigma_\ell = \sigma_m = 0.002$ radian is a one-sigma error of

$$\sigma_n = 0.00088 \text{ radian} \tag{3-32}$$

Assuming that the errors of any beam are statistically independent of the errors of each other beam, the one-sigma value of each element in the error matrix E can be shown to be

$$\Sigma = \begin{bmatrix} \sigma_\ell/2\ell & \sigma_m/2\ell & \sigma_n/2\ell \\ \sigma_\ell/2m & \sigma_m/2m & \sigma_n/2m \\ \sigma_\ell/2n & \sigma_m/2n & \sigma_n/2n \end{bmatrix} \tag{3-33}$$

For the assumed 2 milliradian σ_ℓ and σ_m, these uncompensated one-sigma values are

$$\Sigma = \begin{bmatrix} .0029 & .0029 & .0013 \\ .0050 & .0050 & .0022 \\ .0011 & .0011 & .0005 \end{bmatrix} \qquad (3\text{-}34)$$

The level of these boresight errors is significant, so it is necessary to measure these boresight errors and compensate the measured velocity accordingly. The antenna boresight errors are measured at the factory by Teledyne Ryan as part of the acceptance tests of each unit. This establishes the values of the elements of the error matrix E. The compensation equation is related to the inverse of Equation 3-26, which is approximately

$$\underline{v} = (I - E)\ \hat{\underline{v}} \qquad . \qquad (3\text{-}35)$$

(Note I-E is approximately the inverse of I+E in that $(I+E)(I-E) = I-E^2$, which is the identity matrix to first order.) The one-sigma levels of the compensation matrix elements are the same as given in array 3-34, since the compensation matrix is simply the negative of the error matrix.

The actual compensation equation recommended by Teledyne-Ryan for the APN-200 in use at Holloman AFB is

$$\begin{bmatrix} \hat{v}_h' \\ \hat{v}_d' \\ \hat{v}_z' \end{bmatrix} = \begin{bmatrix} 1+.00271 & 0 & 0 \\ -.00078 & 1-.00658 & 0 \\ -.00146 & 0 & 1+.00016 \end{bmatrix} \begin{bmatrix} \hat{v}_h \\ \hat{v}_d \\ \hat{v}_z \end{bmatrix} \qquad (3\text{-}36)$$

Note the levels of the compensation numbers are consistent with the one-sigma levels based on the 2 milliradian bore-sight-error assumption.

The recommended compensation equation matrix is non-zero only on the main diagonal and the first column. The assumption behind neglecting the other elements is that v_d and v_z are small compared to v_h. However in a high cross wind v_d is not negligible and at a high bank angle in wind v_z is not negligible either.

To analyze the errors of the partial compensation method, denote the error matrix E as being composed of elements to be compensated E^c and elements not to be compensated E^{nc}

$$E = E^c + E^{nc} \tag{3-37}$$

The indicated velocity (Equation 3-26) is

$$\hat{\underline{v}} = (I+E^c+E^{nc})\ \underline{v} \tag{3-38}$$

The compensation (Equation 3-36) is

$$\hat{\underline{v}}' = (I-\hat{E}^c)\ \hat{\underline{v}} \tag{3-39}$$

where $\hat{E}^c$ contains the estimates of the error elements to be compensated. Combining Equation 3-39 and Equation 3-38 and neglecting second order terms, the compensated velocity is

$$\hat{\underline{v}}' = (I+E^c-\hat{E}^c+E^{nc})\ \underline{v} \tag{3-40}$$

The compensated velocity error matrix E' has some elements from the original uncompensated error matrix and some elements which are residual errors after compensation

$$E' = E^c-\hat{E}^c+E^{nc} \tag{3-41}$$

The one-sigma value of each element in the compensated error matrix E' can be shown to be

$$\Sigma = \begin{bmatrix} \sigma_\ell'/2\ell & \sigma_m/2\ell & \sigma_n/2\ell \\ \sigma_\ell'/2m & \sigma_m'/2m & \sigma_n/2m \\ \sigma_\ell'/2n & \sigma_m/2n & \sigma_n'/2n \end{bmatrix} \tag{3-42}$$

where the un-primed sigmas are the uncompensated beam direction-cosine errors and the primed sigmas are the one-sigma direction-cosine errors after compensation. Estimates of the one-sigma errors after compensation are[1]

$$\sigma_\ell' = 0.25 \text{ arc min} = .00007 \text{ radian}$$

$$\sigma_m' = 1.0 \text{ arc min} = .00029 \text{ radian} \tag{3-43}$$

Using Equation 3-31, the third direction-cosine uncertainty after compensation is

$$\sigma_n' = .00007 \text{ radian} \tag{3-44}$$

The one-sigma values of the elements in the compensated error matrix E' (Equation 3-12) are

$$\Sigma = \begin{bmatrix} .00010 & .0029 & .0013 \\ .00017 & .00072 & .0022 \\ .00004 & .0011 & .00004 \end{bmatrix} \tag{3-45}$$

Note that the elements that were not compensated are not necessarily negligible. A large source of error is one that contributes a velocity error that is 0.001 of speed. The column 2 row 1 error is at that level when $v_d = v_h/3$, such as when flying at 300 knots in a 100 knot cross wind.

Only the five calibration numbers shown in Equation 3-29 are encoded in the read only memory of the APN-200. However the other four calibration numbers could be obtained from Teledyne-Ryan. A complete calibration matrix with nine elements would require a negligible increase in computation for the processor using the Doppler data.

3.4.2 Temperature Effect

Thermal expansion of the antenna causes a symmetrical distortion of the beam positions. The temperature coefficient of the direction cosines of the beams is 2.34×10^{-5} per degree C.[1] The radome insulates the antenna from the very large changes in atmosphere temperature from sea-level to altitude. Air from within the aircraft is used to cool the system. A typical deviation of the antenna temperature from the temperature at which the antenna was calibrated would be about 20°C. This would produce a shift in the direction cosines of 0.00047 radian.

The velocity error caused by these direction-cosine errors is also governed by Equation 3-27, whose error matrix E is given in Equation 3-28. Assuming symmetrical distortion of the beam positions ($\delta\ell$'s equal, δm's equal, δn's equal), the error matrix is simply

$$E = \begin{bmatrix} \delta\ell/\ell & 0 & 0 \\ 0 & \delta m/m & 0 \\ 0 & 0 & \delta n/n \end{bmatrix} \qquad (3\text{-}46)$$

Assuming δm equals $\delta\ell$, δn computed from Equation 3-30 must be

$$\delta n = -0.6\ \delta\ell \qquad (3\text{-}47)$$

Then for the assumed one-sigma 20°C temperature deviation, the one-sigma values of the elements of the error matrix are

$$\Sigma = \begin{bmatrix} .0013 & 0 & 0 \\ 0 & .0023 & 0 \\ 0 & 0 & .0003 \end{bmatrix} \qquad (3\text{-}48)$$

This is one of the largest sources of error in the APN-200. For applications where one wishes to reduce this source of error, Teledyne-Ryan recommends mounting a temperature sensor on the antenna and using the temperature data to compensate the indicated velocity.

3.4.3 Installation Alignment

Installation of the unit in the aircraft is referenced to the mounting flange on the radar housing for pitch and roll alignment and to yaw alignment pins in the aircraft which mate with yaw alignment slots in the radar housing. The mating surface of the radar mounting flange has a tolerance of 0.020 inches, which for the 25-inch long surface is equivalent to pitch and roll installation tolerances of 3 arc min.[1]. The yaw alignment pins fit with a tolerance of 0.005 inches in azimuth, which is equivalent to a yaw installation tolerance of 45 arc sec[1]. Assuming a rectangular distribution for the error, between the negative and positive tolerance values, the one-sigma value for the error is 0.58 of the tolerance. In which case, the one-sigma alignment errors are

$$\begin{aligned} \sigma_h &= 1.74 \text{ arc min} = .00051 \text{ rad} \\ \sigma_d &= 1.74 \text{ arc min} = .00051 \text{ rad} \\ \sigma_z &= .43 \text{ arc min} = .00013 \text{ rad} \end{aligned} \qquad (3\text{-}49)$$

The velocity error caused by alignment errors ε_h, ε_d, ε_z can be written in the matrix form (Equation 3-27) where the error matrix in this case is

$$E = \begin{bmatrix} 0 & \varepsilon_z & -\varepsilon_d \\ -\varepsilon_z & 0 & \varepsilon_h \\ \varepsilon_d & -\varepsilon_h & 0 \end{bmatrix} \tag{3-50}$$

From Equation 3-49, the one-sigma values of the elements in the error matrix are

$$\Sigma = \begin{bmatrix} 0 & .00013 & .00051 \\ .00013 & 0 & .00051 \\ .00051 & .00051 & 0 \end{bmatrix} \tag{3-51}$$

3.5 Terrain Bias

The scattering coefficient of the illuminated terrain is a function of the angle of incidence of the radiation. The radiation at the near edge of the beam footprint is steeper than the radiation at the far edge of the beam footprint. The higher scattering coefficient of the near radiation causes a shift in the beam center of power toward the vehicle, as shown in Figure 3-2. For a Doppler sensor that simply tracks the center of power, the shift in direction of center of power causes a velocity error. This effect is called terrain bias.

For typical geometry Doppler sensors in level flight, the error in heading velocity is of the order[2]

$$\delta v_h = .001\ (\Delta\alpha)^2\ m\ v \tag{3-52}$$

where $\Delta\alpha$ is the beamwidth in degrees, m is the slope of the reflectivity curve at the nominal incidence angle in decibels per degree, and v is vehicle velocity.

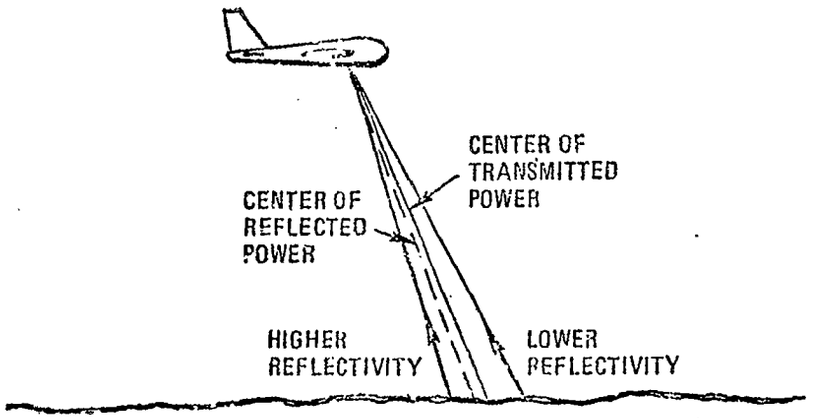

Figure 3-2

Terrain Bias Effect

The reflectivity slope varies greatly between various kinds of terrain, as shown in Figure 3-3 from Reference[1]. Smooth water has the steepest slope. Rough or wooded terrain has the smallest slope. In level flight the beam incidence angle of the APN-200 is 24 degrees. At this angle some of the reflectivity slopes are: .88 db/deg for smooth water, .34 db/deg for smooth barren terrain, .06 db/deg for rough or wooded terrain. For beamwidths of several degrees and for the over-water slope, Equation 3-52 indicates that terrain bias can be a very significant source of error.

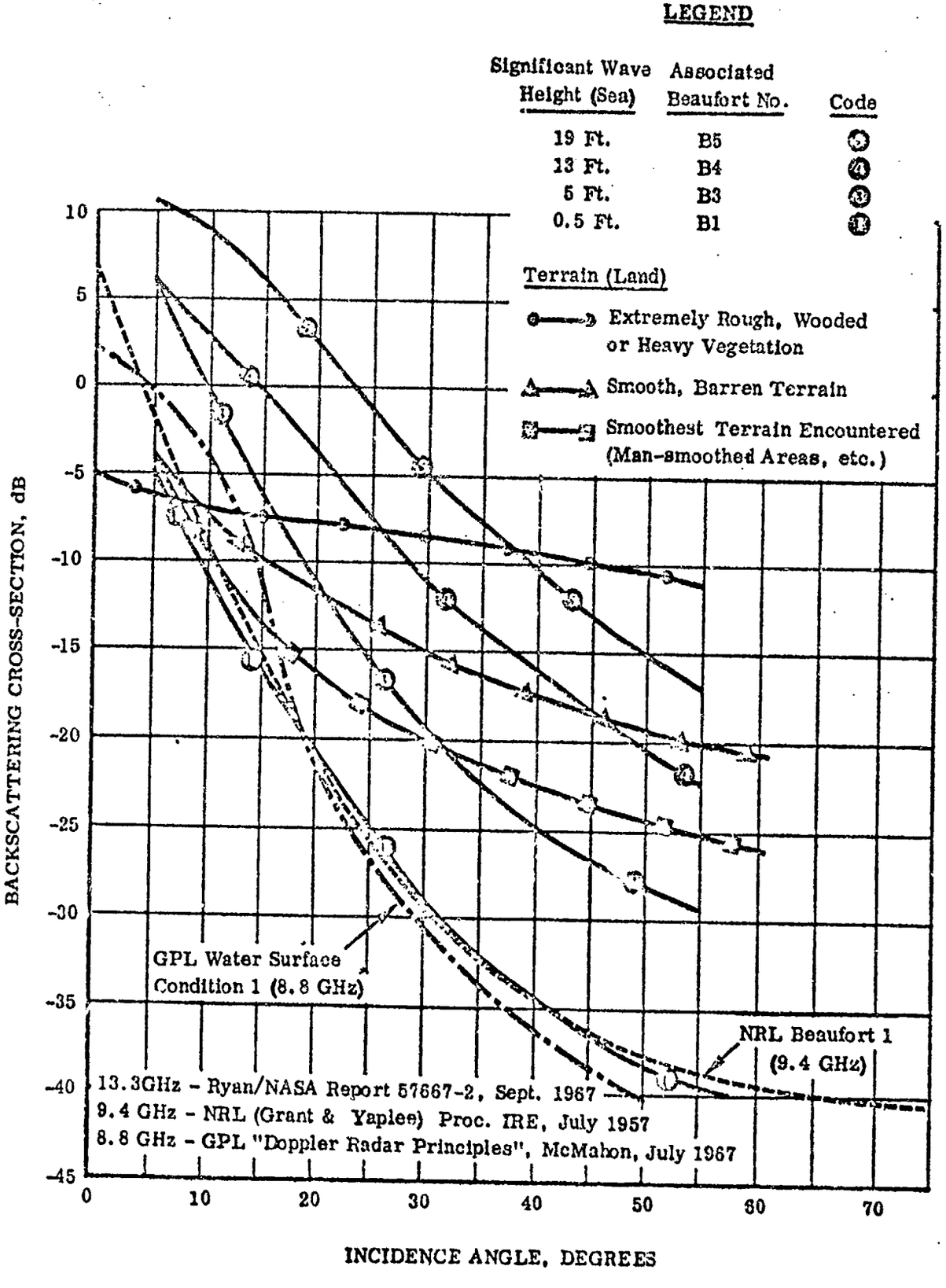

Fig. 3-3 Teledyne Ryan/NASA Reflectivity Data[1]

To suppress the terrain bias effect in the heading component, the APN-200 employs simultaneous lobing as illustrated in Figure 3-4. The difference between the signals received from the two lobes has a null at the Doppler frequency corresponding to the null in the difference radiation pattern. The null frequency and the null direction are not functions of the reflectivity slope. By tracking the null frequency, terrain bias in the heading component is almost eliminated. The finite tracker bandwidth causes some terrain bias effect to remain. The reduction in heading velocity error obtained by lobing techniques is of the order of [2]

$$\delta v_h' / \delta v_h = W_f^2 / \Delta f^2 \tag{3-53}$$

where Δf is the Doppler signal bandwidth and W_f is the lobing low-pass tracker filter bandwidth. The APN-200 Doppler bandwidth at 400 knots is about 550 Hz; while the tracker bandwidth is 60 Hz, so the error reduction is two orders of magnitude. Theoretically, further error reduction could be obtained with a narrower tracker bandwidth. However this would increase the random error variance as was indicated by Equation 3-8.

Because of the four-beam symmetry, in level flight the beam angles of incidence are all 24 degrees. The shifts in direction cosine magnitudes due to terrain bias are the same ($\delta\ell$'s equal, δm's equal, δn's equal). The error in velocity caused by these direction cosine errors is governed by Equation 3-27, whose error matrix E is

$$E = \begin{bmatrix} \delta\ell/\ell & 0 & 0 \\ 0 & \delta m/m & 0 \\ 0 & 0 & \delta n/n \end{bmatrix} \tag{3-54}$$

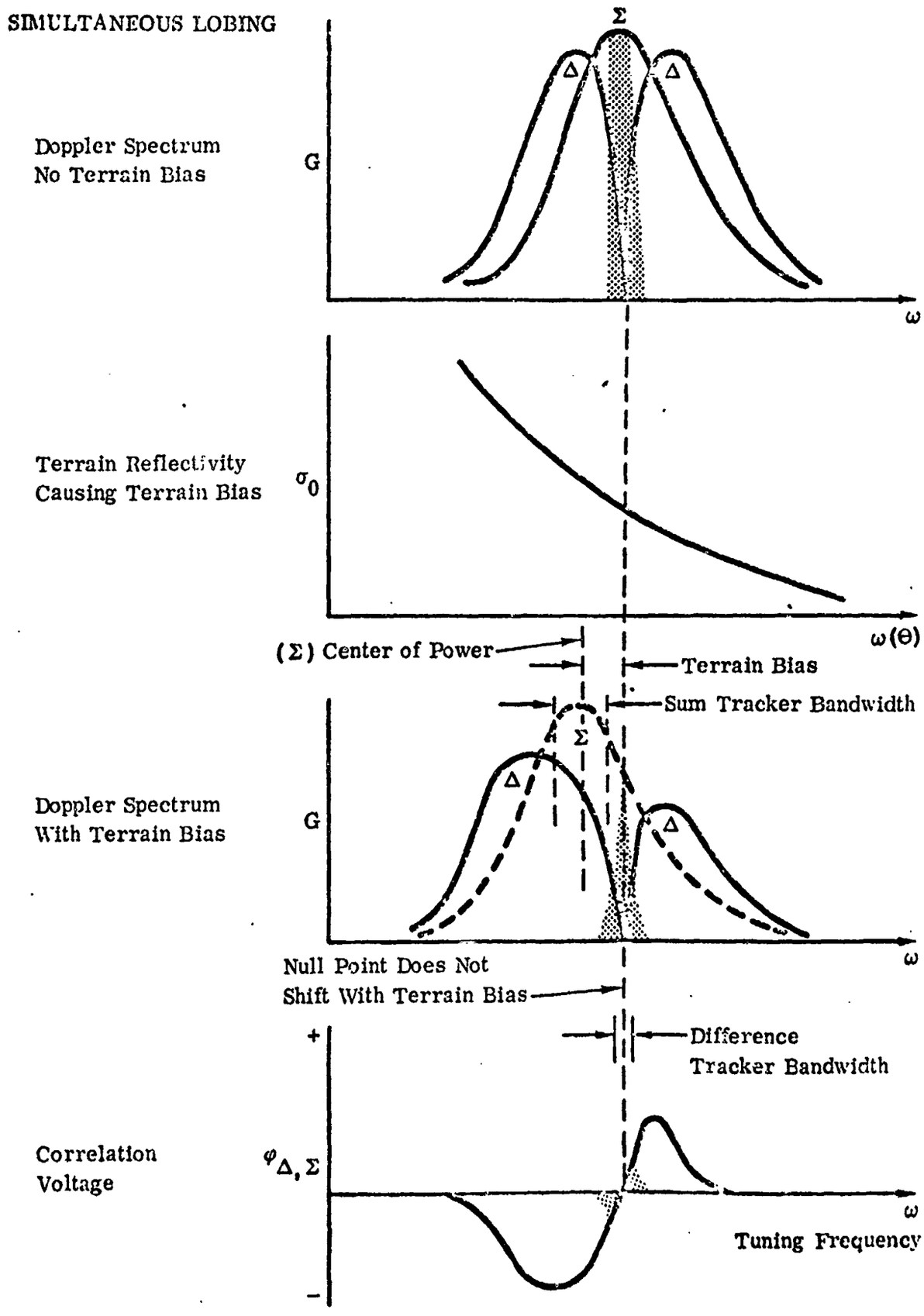

Fig. 3-4 Simultaneous Lobing[1]

Equation 3-54 shows that in level flight, terrain bias causes scale factor errors. Teledyne-Ryan estimates that over smooth water, the heading and drift errors of the APN-200 are[1]

$$\delta v_h = - .00021\ v_h$$

$$\delta v_d = - .0202\ \ v_d \qquad (3\text{-}55)$$

From Equation 3-54, the equivalent direction cosine errors are $\delta\ell$ = -.00007, δm = -.00406 radian. The third direction cosine error from Equation 3-30 must be δn = .00089 radian. So the vertical velocity error over smooth water must be

$$\delta v_z = .00097\ v_z \qquad (3\text{-}56)$$

The values of terrain bias velocity error for three types of terrain are presented in Table 3-1

Terrain	$\delta v_h/v_h$	$\delta v_d/v_d$	$\delta v_z/v_z$
Smooth water	-.00021	-.0202	.00097
Smooth barren terrain	-.00008	-.0079	.00038
Rough or wooded terrain	-.00001	-.0014	.00007

Table 3-1

Terrain Bias Velocity Error

The large over-water lateral error could be compensated in the associated digital computer, provided the computer is told during which portions of the flight the vehicle is over-water. Some residual error would remain due to reflectivity variations as a function of sea state and aircraft pitch and roll. Teledyne-Ryan estimates the residual error would be about one-fourth of the original uncompensated error[1].

The above analysis assumed the aircraft was in level flight. In maneuvering flight at non-zero roll and pitch angles, the angles of incidence of each beam in general are different. This leads to different direction cosine errors for each beam. As a result, according to Equation 3-28, the error matrix is not necessarily diagonal. The E_{zd} coefficient would become significant at non-zero roll angles. The E_{hd} coefficient could be significant at combined non-zero roll and pitch angles.

3.6 Surface Motion

A Doppler velocity sensor measures the velocity of the vehicle relative to the terrain scatterers. Over-water these scatterers may be moving due to sea or river current or due to wind-driven surface motion. Since the velocity of interest is the velocity relative to the fixed earth, surface motion causes a velocity error.

Major ocean currents, such as the Gulf Stream, have a maximum surface speed of about 3 knots. Similar strength currents are observed in coastal areas due to tidal currents. Throughout most of the oceans, general random sea currents rarely exceed 0.5 knot.

Surface-wind water-motion error is caused by wind-blown water particles at and above the surface of the sea. Theoretical analyses and actual measurement of this error have revealed that the velocity error in knots is of the order

$$\delta v = 1.28\ w^{1/3} \qquad (3\text{-}57)$$

where w is the wind velocity in knots.[2] The wind driven spray and therefore the velocity error is roughly parallel to the wind.

3.7 Other Doppler Sources of Error

Several other Doppler sources of error are: transmitter frequency error, receiver sum and difference channel cross coupling, frequency tracker bias, and speed of light in the atmosphere. These sources of error are small compared to the previously discussed errors, so are only briefly discussed in this section.

3.7.1 Transmitter Frequency

The APN-200 transmitter frequency is uncertain within ± 2 MHz of the initial setting and may vary another ± 2 MHz with temperature.[1] Variation in the transmitter frequency from the nominal frequency is directly an error in the assumed Doppler sensitivity. This causes a scale factor error in all velocity components. For the 13.3 GHz transmitter frequency of the APN-200, a 2 MHz frequency error produces scale factor errors of .00015 in all components. The velocity error matrix is

$$E = \begin{bmatrix} .00015 & 0 & 0 \\ 0 & .00015 & 0 \\ 0 & 0 & .00015 \end{bmatrix} \qquad (3\text{-}58)$$

3.7.2 Receiver Cross Coupling[1]

Coupling between the sum and difference channels in the receiver of the APN-200 causes a perturbation in the tracking null point in the simultaneous lobing discriminator. The error has been found to be about 0.03 percent. The resulting heading velocity error is reduced by a factor .707 because the error is the combined effect of the forward and aft receiving channels, which are statistically independent. Drift velocity errors are cancelled because drift velocity is computed as differences of Doppler frequencies processed in the same receiver channels. The errors do not cancel in the computation of v_z. The v_z error is the same as the v_h

error reduced by the ratio of the direction cosines. The velocity error matrix is

$$E = \begin{bmatrix} .00021 & 0 & 0 \\ 0 & 0 & 0 \\ 0 & 0 & .00008 \end{bmatrix} \qquad (3\text{-}59)$$

3.7.3 Frequency Tracker[1]

Frequency tracker errors are specified for the APN-200 as ± 0.05 percent maximum. Assuming a rectangular distribution, this is a one-sigma error of 0.029 percent. This error translates directly into a heading velocity scale factor error. Errors in drift and vertical velocity are practically cancelled because they are computed as differences of the single time-shared tracker output. (Recall as discussed in Section 2.4 that in the APN-200 all Doppler shifts are positive. The heading velocity is computed from the sum of Doppler shifts, whereas the drift and vertical velocities are computed from difference). The velocity error matrix is

$$E = \begin{bmatrix} .00029 & 0 & 0 \\ 0 & 0 & 0 \\ 0 & 0 & 0 \end{bmatrix} \qquad (3\text{-}60)$$

3.7.4 Propagation Velocity

The velocity of the electromagnetic wave in the atmosphere varies as a function of temperature, pressure, and humidity. The velocity at sea level is about 300 parts per million slower than the vacuum velocity. Error in propagation velocity causes scale factor errors in the same way as do frequency drifts. The scale factor error is proportional to the propagation velocity error in the vicinity of the radar set, since the local wavelength determines the Doppler scale factor. The APN-200 scale factor is based on the wavelength at 40,000 feet. At sea level the scale factor error would be .0003. The velocity error matrix at sea level is

$$E = \begin{bmatrix} .0003 & 0 & 0 \\ 0 & .0003 & 0 \\ 0 & 0 & .0003 \end{bmatrix} \qquad (3\text{-}61)$$

Using a standard exponential atmosphere model, this error could be calibrated to an accuracy of about 50 parts per million.

3.8 Non-Doppler Attitude Errors

3.8.1 Definitions

To be useful for navigation, the aircraft-referenced measured velocity components must be transformed to navigation-frame coordinates (such as an east-north-down set). This may be indicated by

$$\hat{v}^n = \hat{C}_d^n \hat{v}^d \qquad (3\text{-}62)$$

where $\hat{v}^d$ is the measured velocity in Doppler (aircraft) coordinates, $\hat{C}_d^n$ is the computed transformation to navigation-frame from Doppler-frame coordinates and $\hat{v}^n$ is the computed velocity in navigation frame coordinates. A first order analysis of the error in the computed velocity δv^n shows that

$$\delta v^n = C_d^n \delta v^d + \delta C_d^n v^d \qquad (3\text{-}63)$$

That is, in addition to the Doppler equipment and environment errors giving rise to the Doppler velocity error in Doppler coordinates δv^d there is also velocity error due to the in the attitude transformation δC_d^n.

Of particular interest are the errors in attitude using a gimballed inertial navigation system (INS) as the attitude reference. The transformation matrix C_d^n to navigation-frame from Doppler-frame coordinates is the product of three distinct transformations.

$$C_d^n = C_p^n C_b^p C_d^b \qquad (3\text{-}64)$$

C_p^n is the transformation to navigation-frame from INS stable-platform coordinates, C_b^p is the transformation to stable-platform from INS-base-plate coordinates, and C_d^b is the transformation to INS-base-plate from Doppler-base-plate coordinates. Errors in the measured or computed estimates of each of these three transformations contribute to the total attitude transformation error.

Assuming small attitude errors, each computed transformation matrix may be expressed in terms of true transformation matrix and an error matrix as

$$\hat{C}_i^j = C_i^j \ (I+E_{ji}{}^i) \tag{3-65}$$

where $E_{ji}{}^i$ is a skew-symmetric attitude-error matrix whose three independent elements are elements of a small-angle rotation vector in i-frame coordinates. A first order analysis of the error in the total attitude transformation shows that

$$\delta C_d^n = C_d^n \ (E_{np}{}^d + E_{pb}{}^d + E_{bd}{}^d) \tag{3-66}$$

where $E_{np}{}^d$ is the attitude error matrix associated with the to-n-from-p transformation but transformed to the Doppler coordinates d, and the other two attitude error matrices are similarly defined.

In this report we have been focussing attention on the velocity errors in Doppler (aircraft) coordinates. The error in computed velocity given by Equation 3-63 may be transformed back to Doppler coordinates, and the term expressing the velocity error due to attitude error is then seen to be of the form

$$\delta v = E \ v^d \tag{3-67}$$

where

$$E = E_{np}{}^d + E_{pb}{}^d + E_{bd}{}^d \tag{3-68}$$

3.8.2 INS Stable Platform Attitude Error

The first of three transformations in Eq. (3-64) is the transformation to navigation from platform coordinates. The inertial navigation computer maintains an estimate of this transformation, based on a knowledge of the angular velocity of the navigation frame and a knowledge of the angular velocity commands (gyro torquer commands) to the gyro-stabilized platform. The error in the computed transformation gives rise to the velocity error matrix (in Eq. 3-68) of the form

$$E_{np}^{d} = \begin{bmatrix} 0 & \varepsilon_z & -\varepsilon_d \\ -\varepsilon_z & 0 & \varepsilon_h \\ \varepsilon_d & -\varepsilon_h & 0 \end{bmatrix} \qquad (3\text{-}69)$$

where ε_h, ε_d, ε_z are the three components of the (small angle) INS attitude error vector. The sign convention of each component is that the attitude error about a given axis is positive if the platform is rotated positively (by the right hand rule) about that axis relative to the INS-computed platform orientation with respect to the navigation frame.

The magnitudes of these attitude errors depend on the manner in which the INS is initially aligned, the quality of the inertial instruments (gyros and accelerometers), and on the flight path trajectory and duration. For a high quality INS, aligned by self-leveling and gyrocompassing, after several hours of subsonic flight, the horizontal components of attitude error will be of the order of one arc min and the azimuth error will be of the order of several arc min.

In an optimal integration of the Doppler system with an inertial system, the three INS attitude error components would be included in the state vector of the Kalman filter. These error components are time varying. The set of differential equations governing the INS error state (including attitude, velocity, and position errors) may be found in the literature on inertial navigation system analysis.

Pitman[6] provides an introduction. Britting[7] presents a more general and advanced treatment. Widnall and Grundy[8] present general INS error models in the modern state space formulation.

3.8.3 INS Attitude Readout Error

The second transformation in Eq. (3-64) is the transformation to platform from INS-base-plate coordinates. An estimate of this transformation is computed from the measured INS gimbal angles. The error in the computed transformation gives rise to a velocity error matrix of the same form

$$E_{pb}^{d} = \begin{bmatrix} 0 & \varepsilon_z & -\varepsilon_d \\ -\varepsilon_z & 0 & \varepsilon_h \\ \varepsilon_d & -\varepsilon_h & 0 \end{bmatrix} \tag{3-70}$$

where ε_h, ε_d, ε_z have represent components of the attitude readout error. A component is positive about an axis if the base-plate is rotated positively about that axis relative to the measured base-plate orientation with respect to the platform.

The gimbal angles are (in a typical INS) measured by electrical resolvers. The resolver error can be of the order of several arc min. In the Litton CAINS platform (utilized in the Holloman AFB CIRIS system), there are single-speed resolvers for pitch and roll of accuracy 2.5 arc min 1σ, and there is an eight-speed resolver for azimuth of accuracy .75 arc min 1σ. In level flight, these resolver errors transform into attitude readout components having one-sigma values

$$\begin{aligned} \sigma_h &= 2.5 \text{ arc min} = .00073 \text{ rad} \\ \sigma_d &= 2.5 \text{ arc min} = .00073 \text{ rad} \\ \sigma_z &= .75 \text{ arc min} = .00022 \text{ rad} \end{aligned} \tag{3-71}$$

The corresponding one-sigma values of the elements in the velocity error matrix are

$$\Sigma = \begin{bmatrix} 0 & .00022 & .00073 \\ .00022 & 0 & .00073 \\ .00073 & .00073 & 0 \end{bmatrix} \qquad (3\text{-}72)$$

Resolver error is constant at a constant aircraft attitude. But when the aircraft attitude changes, the resolver error also changes.

An additional source of error, which may be considered part of the INS attitude readout error, is the difference in alignment between the platform true horizontal axes and the accelerometer-defined horizontal axes. The INS is leveled during alignment by nulling the outputs of the two horizontal accelerometers. However, because of several physical effects (accelerometer input axis misalignment, accelerometer bias, gravity deflection), the platform alignment that nulls the accelerometer outputs is not truely level. This bias in platform attitude error, while having no significant effect on INS navigation accuracy, does directly contribute to INS attitude readout error. In a high quality inertial system (small accelerometer input axis misalignments and biases) the bias platform attitude error should be less than one arc min, which may be neglected compared with the pitch and roll resolver errors. For an INS for which the bias attitude error is not negligible, it should be noted that constant platform attitude errors in east-north coordinates take on varying values in aircraft coordinates as heading changes.

3.8.4 INS-Doppler Installation Alignment

The last of the three transformations in Eq. (3-64) is the transformation to INS-base-plate from Doppler-base-plate

coordinates. If both the Doppler and INS base plates are nominally aligned with the aircraft coordinate axes, this transformation is nominally the identity matrix. The error in the assumed transformation gives rise to a velocity error matrix of the same form

$$E_{bd}^{d} = \begin{bmatrix} 0 & \varepsilon_z & -\varepsilon_d \\ -\varepsilon_z & 0 & \varepsilon_h \\ \varepsilon_d & -\varepsilon_h & 0 \end{bmatrix} \qquad (3\text{-}73)$$

where ε_h, ε_d, ε_z here represent components of the installation alignment error vector. A component is positive about an axis if the Doppler base-plate is rotated positively about that axis relative to the nominal or measured Doppler base-plate orientation with respect to the INS base-plate.

Sources of installation alignment error include the initial alignment error (on the ground) plus the subsequent bending of the aircraft, due to changes in structural, aerodynamic, and thermal loads. A very rough estimate of the in-flight installation alignment errors is

$$\begin{aligned} \sigma_h &= 5 \text{ arc min} = .0015 \text{ rad} \\ \sigma_d &= 10 \text{ arc min} = .0029 \text{ rad} \\ \sigma_z &= 2 \text{ arc min} = .0006 \text{ rad} \end{aligned} \qquad (3\text{-}74)$$

The corresponding one-sigma values of the elements in the velocity error matrix are

$$\Sigma = \begin{bmatrix} 0 & .0006 & .0029 \\ .0006 & 0 & .0015 \\ .0029 & .0015 & 0 \end{bmatrix} \qquad (3\text{-}75)$$

At a given flight condition, the INS-to-Doppler installation alignment error should be constant. But changes in speed, altitude, or maneuvering loads will change the structural, aerodynamic, and thermal loads, thereby changing the alignment error.

3.9 Combined Velocity Error Matrix

In the preceeding sections, the various sources of Doppler velocity error were discussed. Most sources of error were shown to contribute to velocity error in a manner proportional to vehicle velocity according to the matrix equation

$$\delta \underline{v} = E \, \underline{v}$$

$$\begin{bmatrix} \delta v_h \\ \delta v_d \\ \delta v_z \end{bmatrix} = \begin{bmatrix} E_{hh} & E_{hd} & E_{hz} \\ E_{dh} & E_{dd} & E_{dz} \\ E_{zh} & E_{zd} & E_{zz} \end{bmatrix} \begin{bmatrix} v_h \\ v_d \\ v_z \end{bmatrix} \qquad (3\text{-}76)$$

The only velocity errors not related to their sources in the above manner were: 1) the noise due to finite beamwidth, 2) error due to tracker time constant when the vehicle is maneuvering, and 3) error due to surface motion.

Table 3-2 summarizes the sources of error which contribute to velocity error according to Eq. (3-76). The table shows the one-sigma value of each element of the velocity error matrix for each source of error. The total velocity error due to all of these sources of error is also governed by an error equation of the form Eq. (3-76), where each element of the velocity error matrix is the sum of the corresponding elements of the individual error matrices. Assuming all sources of error are statistically independent, the one-sigma value of each element in the combined velocity error matrix is the root sum square of the individual one-sigma values. These root-sum-square values are given at the bottom of the table.

Error Source	Assumption	Error Characteristic	E_{hh}	E_{hd}	E_{hz}	E_{dh}	E_{dd}	E_{dz}	E_{zh}	E_{zd}	E_{zz}
Beam Direction Errors											
Residual Errors after Compensation	Not all elements are compensated	Constant	.00010	.00290	.00130	.00017	.00072	.00220	.00004	.00110	.00004
Temperature Effect	-	Slowly varying	.00130	0	0	0	.00230	0	0	0	.00030
Installation Alignment	-	Constant	0	.00013	.00051	.00013	0	.00051	.00051	.00051	0
Terrain Bias	Level flight over smooth barren terrain	Varies with attitude and terrain	.00008	0	0	0	.00790	0	0	0	.00038
Transmitter Frequency	-	Slowly varying	.00015	0	0	0	.00015	0	0	0	.00015
Receiver Cross Coupling	-	Constant	.00021	0	0	0	0	0	0	0	.00008
Frequency Tracker	-	Slowly Varying	.00029	0	0	0	0	0	0	0	0
Propagation Velocity	Near sea level	Varies with altitude	.00030	0	0	0	.00030	0	0	0	.00030
Non-Doppler Attitude Errors											
INS Attitude Readout Error	Level flight	Varies with attitude and heading	0	.00022	.00073	.00022	0	.00073	.00073	.00073	0
INS-Doppler Installation Alignment	-	Varies with speed, altitude, and maneuvers	0	.00060	.00290	.00060	0	.00150	.00290	.00150	0
Combined Velocity Error Matrix Elements (Root Sum Square of All Sources)			.00140	.00297	.00330	.00067	.00823	.00281	.00303	.00206	.00059

Table 3-2 Velocity Error Matrix Elements Due to all Sources (One-Sigma Values)

... METRICS INCORPORATED • 701 CONCORD AVENUE • CAMBRIDGE, MASSACHUSETTS 02138 • (617) 661-...

Any element of the table exceeding one mil (.00100) is circled, to point out the most significant sources of error.

Note that INS stable platform attitude error is not included in the table. It is usually accounted for separately.

3.10 Doppler Error Model Summary

The error $\delta\underline{v}$ in vehicle velocity, measured by the APN-200 Doppler velocity sensor and resolved into navigation frame coordinates according to the INS-indicated attitude, may be summarized by the following equation:

$$\delta\underline{v} = E\,\underline{v} + E_I\,\underline{v} + \delta\underline{v}_\tau + \delta\underline{v}_s + \underline{w} \qquad (3\text{-}77)$$

where

E = combined velocity error matrix (excluding INS attitude error)

E_I = velocity error matrix due to INS attitude error

$\delta\underline{v}_\tau$ = velocity error due to tracker time constant

$\delta\underline{v}_s$ = velocity error due to surface motion

$\underline{w}$ = noise due to finite beamwidth

All vectors in Eq. (3-77) are assumed to be expressed in Doppler antenna coordinates (or equivalently in aircraft coordinates), for which the three components are in the heading (forward), drift (right), and vertical (down) directions.

The noise vector $\underline{w}$ due to finite beamwidth, as discussed in Section 3.2, has covariance matrix R specified as being less than

$$R = v \begin{bmatrix} .016 & 0 & 0 \\ 0 & .031 & 0 \\ 0 & 0 & .008 \end{bmatrix} \qquad (3\text{-}78)$$

where v is in knots to obtain velocity error variance R in knots^2. The noise components are uncorrelated with each other. Each noise component has a short correlation time, of the order of the 0.2 sec Doppler output time constant.

The combined velocity error matrix E is of the form

$$E = \begin{bmatrix} E_{hh} & E_{hd} & E_{hz} \\ E_{dh} & E_{dd} & E_{dz} \\ E_{zh} & E_{zd} & E_{zz} \end{bmatrix} \qquad (3\text{-}79)$$

In level flight over smooth barren terrain, the one-sigma values of the error matrix elements are, according to Table 3-2

$$\Sigma = \begin{bmatrix} .00140 & .00297 & .00330 \\ .00067 & .00823 & .00281 \\ .00303 & .00206 & .00059 \end{bmatrix} \qquad (3\text{-}80)$$

The elements of the velocity error matrix in level flight are generally constant or slowly varying. However, the element E_{dd}, which is dominated by lateral terrain bias, can shift suddenly if the terrain changes suddenly.

In maneuvering flight, some of the elements of the velocity error matrix E will have larger one-sigma values than those given in Eq. (3-80).

The velocity error matrix E_I due to inertial navigation system attitude error is, as was given in Eq. (3-69)

$$E_I = \begin{bmatrix} 0 & \varepsilon_z & -\varepsilon_d \\ -\varepsilon_z & 0 & \varepsilon_h \\ \varepsilon_d & -\varepsilon_h & 0 \end{bmatrix} \qquad (3\text{-}81)$$

where ε_h, ε_d, ε_z are the three components of the (small angle) INS attitude error vector in aircraft coordinates.

The velocity error due to tracker time constant was discussed in Section 3.3. It is significant only during maneuvering flight when beam velocity components are changing.

The velocity error due to surface motion was discussed in Section 3.6. Over water, surface motion may be present due to current or wind driven surface velocity. When present (over water) this source of error can be very significant.

3.11 Error Model Simplifications for Kalman Filter Synthesis

To design a Kalman filter for mixing Doppler velocity measurements with velocity from an inertial navigation system, the designer must select an appropriate statistical model for the Doppler velocity errors. It is usually possible to simplify the complete error model of Eq. (3-77) without causing significant loss of accuracy with respect to the theoretically optimal performance.

Over land, the surface motion term is zero, so may be discarded. The tracker time constant term is very small during non-accelerated flight, so may be discarded in cruise navigation applications.

The velocity error matrix E_I due to INS attitude error has three independent elements (Eq. 3-81) which are the three components of the (small angle) INS attitude error. If the Kalman filter is supposed to improve the knowledge of the INS attitude error, then the INS attitude error term must be retained in the Doppler measurement error model.

The combined velocity error matrix E (excluding INS attitude error) has nine independent elements, whose one-sigma values were presented in Eq. (3-80). One could include all nine elements of the error matrix as state variables in the Kalman filter. However, it seems reasonable that no more than three state variables are required to model the slowly varying velocity error. The three state variables can be directly the components of velocity error δv_h, δv_d, δv_z.

A better choice, however, is the set of non-dimensional parameters $\delta v_h/v_h$, $\delta v_d/v_h$, $\delta v_z/v_h$. This latter choice is motivated by the fact that for small drift velocity and vertical velocity, the ratio parameters are constant or slowly varying, independent of speed. The velocity error variables, on the other hand, can change directly with any speed change.

The first state variable $\delta v_h/v_h$ will be essentially equivalent to the velocity error matrix element E_{hh}. This follows from the data in Eq. (3-80), which show one-sigma values of the three elements contributing to the ahead velocity error are σ_{hh} = .00140, σ_{hd} = .00297, and σ_{hz} = .00330. For typical values of drift velocity and vertical velocity, the contributions of E_{hd} and E_{hz} to forward velocity error will be smaller than the contribution of E_{hh}. Thus, forward velocity error is most nearly a scale-factor error.

The second state variable $\delta v_d/v_h$ is not clearly related to a single element in the velocity error matrix. If there is small drift velocity, the drift velocity error will be related to the forward velocity according to the matrix element E_{dh}. This has the characteristic of an azimuth alignment error. But if the drift velocity is large, the dirft velocity error will be related to the drift velocity according to the matrix element E_{dd}. This is a lateral scale factor error. From the data in Eq. (3-80), showing one-sigma values of σ_{dh} = .00067 and σ_{dd} = .00823, the two error elements are of equal significance when drift velocity is 8% of forward velocity.

The third state variable $\delta v_z/v_h$ will be essentially equivalent to the velocity matrix element E_{zh}. The data in Eq. (3-80) show that for typical values of drift and vertical velocity, the contributions of the other two elements E_{zd} and E_{zz} are negligible. Thus, the vertical velocity error is most nearly a pitch alignment error.

Each of the three state variables can be modeled as being governed by a first-order Markov process of the form

$$\dot{x} = -\frac{1}{\tau}x + w \qquad (3\text{-}82)$$

where the time constant τ is selected to model the slowly varying character of the state variable and the white noise w is assigned a spectral density N appropriate to maintain the assumed one-sigma amplitude of the state variable.

In some applications, only horizontal navigation is of interest, in which case the third (vertical) component of the Doppler velocity may be discarded. Accordingly, in these applications, only two state variables need be included in the Kalman filter, representing the slowly varying error in heading velocity and drift velocity.

CHAPTER 4

ANALYSIS OF FLIGHT TEST DATA

4.1 Introduction

Performance parameters for modelling the Teledyne-Ryan APN-200 Doppler velocity sensor were obtained by reducing flight test data recorded during a single 2-1/2 hour flight over the Tularosa Basin on 7 August 1973.

The aircraft ground track is sketched in Figure 4-1. It takes-off from Holloman Air Force Base and flies west to the -106.35° longitude line, while gaining altitude. It then turns north and climbs to 32,000 feet. The aircraft turns to the southwest, and after a couple of minutes, turns to the southeast and flies back to the -106.35° longitude. It proceeds south at this longitude for approximately 8 minutes, after which it executes a left turn and flies back north at the same longitude. The aircraft flies two more courses over this path, after which it returns and lands at Holloman. During the flight, the Doppler velocity measurements to be used for data reduction are recorded at the nominal rate of once/second.

In addition to the APN-200, the aircraft was equiped with a CAINS baro-inertial navigation system and a CR-100 range/delta-range measuring system. Four transponders were deployed on the ground for ranging purposes: at Holloman (#4), at Sunspot (#6), at Stallion Army Base (#8) and at Salt Creek (#9) in the White Sands Missile Range, as also marked in Figure 4-1. The CAINS and CR-100 recorded outputs were processed by the CIRIS Post-Flight-Processor (PFP)[5] to generate optimal estimates of the aircraft's velocity at the Doppler measurement times. These estimates were subtracted from the Doppler indicated velocities to generate measurement residuals, which were then statistically processed to compute estimates of the Doppler error coefficients.

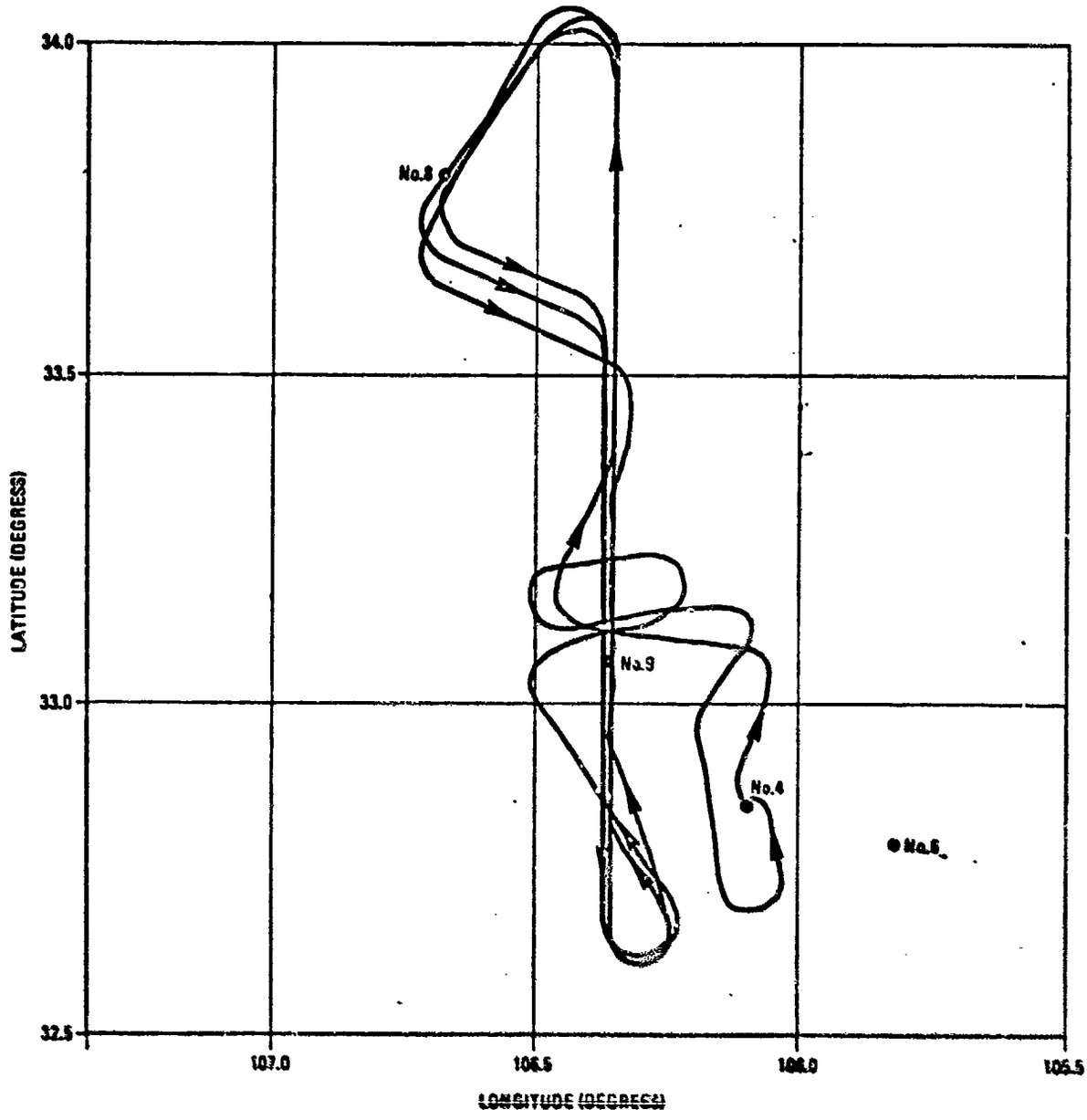

Fig. 4-1 Aug 7 Plight Ground Track

4.2 Isolation of Doppler Sensor Errors

In order to obtain the Doppler errors, the true aircraft velocity must be subtracted from the measurements. The CIRIS PFP contains a two-pass "optimal" smoother, which provides a velocity reference accurate to the order of .1 ft/sec. Figures 4-2 and 4-3 exhibit the smoother-computed one-sigma uncertainties in the estimated velocity in geographic axes. If the CAINS inertial system and the CR-100 precision ranging system are performing according to their performance specifications as accounted for in the optimal smoother, then the smoother computed uncertainties may be interpreted as the reference system accuracy.

The estimated velocity must be transformed to aircraft axes for comparison with the Doppler measurements. This transformation is effected through the CAINS platform gimbal angles, corrected by the smoother estimated platform attitude errors, as given by

$$C_n^a = C_p^a \, C_{n_c}^p \, C_n^{nc} \qquad (4\text{-}1)$$

where

C_n^a = coordinate transformation matrix from geographic coords (East, North, Up) to aircraft axes (Roll, Pitch, Yaw)

C_p^a = coordinate transformation matrix from CAINS platform coords (X, Y, Z) to aircraft axes, through the platform gimbal angles

$C_{n_c}^p$ = coordinate transformation matrix from CAINS estimated geographic frame to platform coordinates, through the wander azimuth angle

C_n^{nc} = coordinate transformation matrix from geographic coords to CAINS estimated geographic coords, through the smoother platform attitude errors

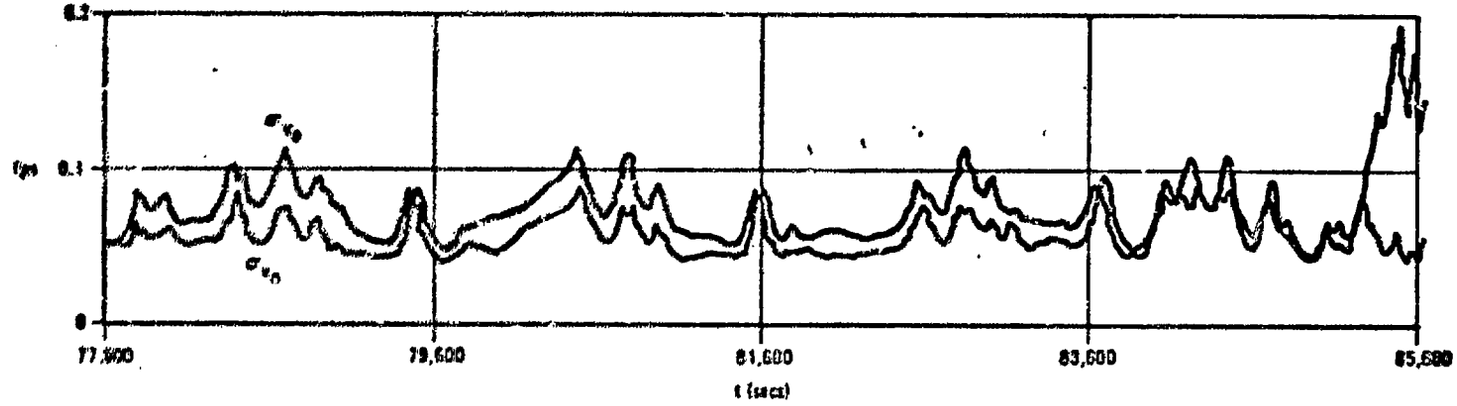

Fig. 4-2 Reference System Horizontal Velocity 1σ Error (Computed by PFP Smoother)

INTERMETRICS INCORPORATED • 701 CONCORD AVENUE • CAMBRIDGE, MASSACHUSETTS 02138 • (617) 661-1

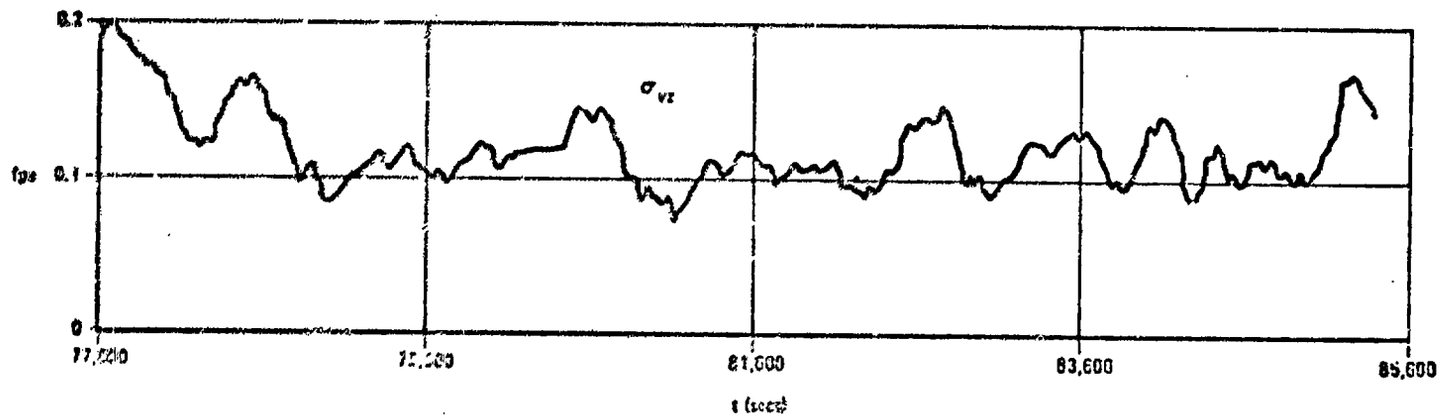

Fig. 4-3 Reference System Vertical Velocity 1σ Error
(Computed by PFP Smoother)

Thus,

$$C_p^a = \begin{bmatrix} \cos\theta\sin\psi_p & \cos\theta\cos\psi_p & \sin\theta \\ \sin\phi\sin\theta\sin\psi_p + \cos\phi\cos\psi_p & \sin\phi\sin\theta\cos\psi_p - \cos\phi\sin\psi_p & -\sin\phi\cos\theta \\ \cos\phi\sin\theta\sin\psi_p - \sin\phi\cos\psi_p & \cos\phi\sin\theta\cos\psi_p + \sin\phi\sin\psi_p & -\cos\phi\cos\theta \end{bmatrix} \quad (4\text{-}2)$$

where

ϕ = roll gimbal angle

θ = pitch gimbal angle

ψ_p = azimuth gimbal angle,

$$C_{n_c}^p = \begin{bmatrix} \cos\alpha & \sin\alpha & 0 \\ -\sin\alpha & \cos\alpha & 0 \\ 0 & 0 & 1 \end{bmatrix} \quad (4\text{-}3)$$

where

α = wander azimuth angle,

and, making small angle assumptions for the platform attitude errors

$$C_n^{n_c} = \begin{bmatrix} 1 & \varepsilon_z & -\varepsilon_n \\ -\varepsilon_z & 1 & \varepsilon_e \\ \varepsilon_n & -\varepsilon_e & 1 \end{bmatrix} \quad (4\text{-}4)$$

where

ε_e = platform tip about east

ε_n = platform tip about north

ε_z = platform azimuth error

The platform tips about east and north can be neglected based on the following considerations: they are consistently less than 1 minute throughout the flight, and hence their effect on the desired residuals will be an order of magnitude below the Doppler induced errors; their effect on the along and cross heading velocity estimates is through the vertical velocity, which is well below horizontal speeds. The platform azimuth error, the largest of the three, and furthermore, directly incident on the Doppler boresight error, will be included in the transformation. Hence, the resulting transformation matrix is given by

$$C_n^a = \begin{bmatrix} \cos\theta\sin\psi & \cos\theta\cos\psi & \sin\theta \\ \sin\phi\sin\theta\sin\psi + \cos\phi\cos\psi & \sin\phi\sin\theta\cos\psi - \cos\phi\sin\psi & -\sin\phi\cos\theta \\ \cos\phi\sin\theta\sin\psi - \sin\phi\cos\psi & \cos\phi\sin\theta\cos\psi + \sin\phi\sin\psi & -\cos\phi\cos\theta \end{bmatrix} \quad (4\text{-}5)$$

where

$\psi = \psi_p - \alpha - \varepsilon_z$ = aircraft heading

The estimated velocity in aircraft axes is then given by

$$\hat{\underline{v}}^a = C_n^a \hat{\underline{v}}^n \quad (4\text{-}6)$$

where

$\hat{\underline{v}}^a$ = estimated velocity in aircraft axes

$\hat{\underline{v}}^n$ = estimated velocity in geographic axes

The CAINS indicated velocity contains a deterministic error resulting from what appear to be out of specification accelerometer scale factors. This error has been compensated in the PFP by the following expressions

$$e_{v_e} = e_{v_e} + ASF_x \cdot f_{int_x} \cdot \cos(\alpha) - ASF_y \cdot f_{int_y} \cdot \sin(\alpha)$$

$$+ YAZ \cdot f_{int_x} \cdot \sin(\alpha)$$

$$e_{v_n} = e_{v_n} + ASF_x \cdot f_{int_x} \cdot \sin(\alpha) + ASF_y \cdot f_{int_y} \cdot \cos(\alpha)$$

$$- YAZ \cdot f_{int_x} \cdot \cos(\alpha) \qquad (4\text{-}7)$$

where

e_{v_e} = error in east velocity (CAINS-true)

e_{v_n} = error in north velocity (CAINS-true)

f_{int_x} = integral of specific force along platform X axis (X accel.)

f_{int_y} = integral of specific force along platform Y axis

α = platform wander angle

and

ASF_x = X accelerometer scale factor = 4000 ppm

ASF_y = Y accelerometer scale factor = -4900 ppm

ASF_z = Y accelerometer misalignment about Z platform axis = - 1 min

The smoothed velocity is provided by the PFP at the CAINS read times, which are synchronized with doppler measurements. The doppler residuals are then generated by differencing the estimates from the doppler velocities in aircraft coordinates

$$\delta\underline{v}^a = \underline{v}_m^a - \hat{\underline{v}}^a \tag{4-8}$$

where

$\delta\underline{v}^a$ = doppler measurement residuals in aircraft axes

$\hat{\underline{v}}_m^a$ = measured doppler velocity in aircraft axes

A contributor to the above difference between IMU/PFP derived velocity and doppler measured velocity is the relative velocity due to the fact that the doppler antenna is not co-located with the IMU. Aircraft attitude rates will induce additional velocity at the antenna, proportional to the IMU-to-antenna lever arm, i.e.,

$$\delta\underline{v}^a = \underline{\omega}^a \times \underline{R}^a \tag{4-9}$$

where

$\delta\underline{v}^a$ = antenna lever arm induced velocity increments

$\underline{\omega}^a$ = attitude rate in aircraft axes

$\underline{R}^a$ = antenna lever arm in aircraft axes

and

$$\underline{\omega}^a = \begin{bmatrix} \dot{\phi} - \dot{\psi}\sin\theta \\ \dot{\theta}\cos\phi + \dot{\psi}\cos\theta\sin\phi \\ -\dot{\theta}\sin\phi + \dot{\psi}\cos\theta\cos\phi \end{bmatrix} \tag{4-10}$$

with

ϕ = roll angle

θ = pitch angle

ψ = heading angle

and $\dot{()}$ indicates a time derivative.

In the test aircraft, the antenna lever arm was

$$\underline{R}^a = \begin{bmatrix} 10.666 \\ 0. \\ 3.58 \end{bmatrix} \quad . \tag{4-11}$$

Hence

$$\delta\underline{v}^a = \begin{bmatrix} (\dot{\theta}\cos\phi + \dot{\psi}\cos\theta\sin\phi) \cdot 3.58 \\ (-\dot{\theta}\sin\phi + \dot{\psi}\cos\theta\cos\phi) \cdot 10.666 - (\dot{\phi} - \dot{\psi}\sin\theta) \cdot 3.58 \\ -(\dot{\theta}\cos\phi + \dot{\psi}\cos\theta\sin\phi) \cdot 10.666 \end{bmatrix} \tag{4-12}$$

The only persistent attitude rate is the heading rate $\dot{\psi}$. For coordinated turns at 30° bank angle, at a speed of 600 ft/sec, this angular velocity is of the order of .03 rad/sec, which, at zero pitch angle, induces velocities of

$$\delta\underline{v}^a = \begin{bmatrix} .055 \\ .34 \\ -.165 \end{bmatrix} \quad \text{ft/sec} \tag{4-13}$$

These components of relative velocity are sufficiently small (compared to other sources of Doppler velocity error) so that an antenna lever arm correction is not required.

The set of non-dimensional error variables $\delta v_h/v_h$, $\delta v_d/v_h$, $\delta v_z/v_h$ is selected for statistical analysis. As discussed in Section 3.11, these variables may be constant or slowly varying independent of speed. Symbol definitions are

δv_h = along heading doppler measurement residual

δv_d = cross heading (drift) doppler measurement residual

δv_z = along yaw axis doppler measurement residual

and

v_h = along heading doppler velocity

v_h is plotted in Fig. 4-4 with flight events marked, while the doppler residual ratios are plotted in Figs. 4-5, 4-6, and 4-7 respectively. For purposes of readability, only every fifth available point was plotted. Also, overlayed on these, is a graph of the sample mean computed using the nearest 100 samples.

4.3 Segment Selection for Statistical Analysis

In order to obtain a measure of the variability of the doppler errors statistical parameters, it is desirable to break up the available flight data into time segments, each of which is to be reduced separately. The segment selection is based on the following considerations:

a) Flight Path - the selected segments should not contain samples pertaining to different conditions, i.e., samples obtained over land should not be mixed with samples obtained over water (if there were any), straight and level flight portions should not be mixed with maneuvering segments or with altitude transitions, etc.

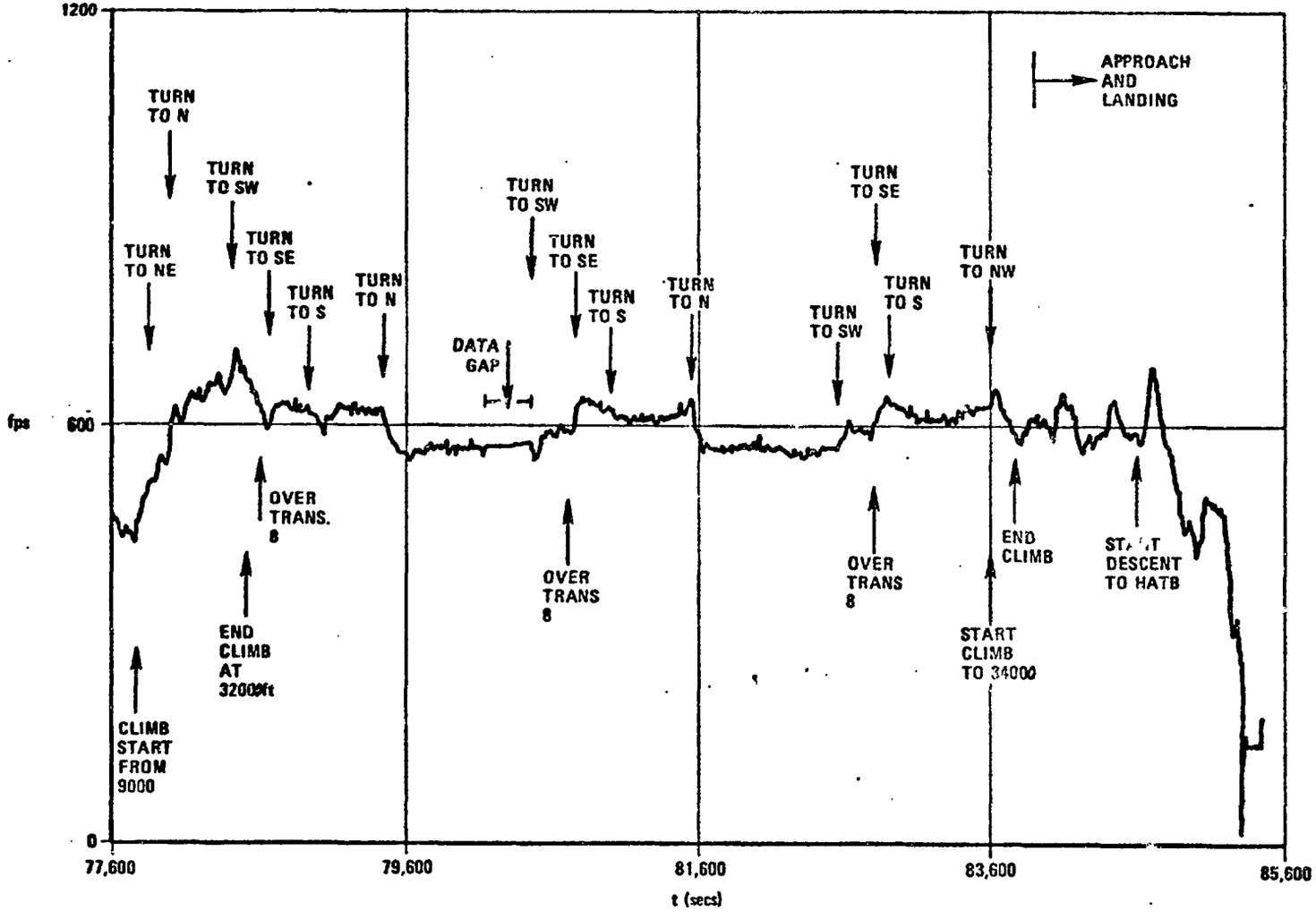

Fig. 4-4 Heading Velocity and Flight Events

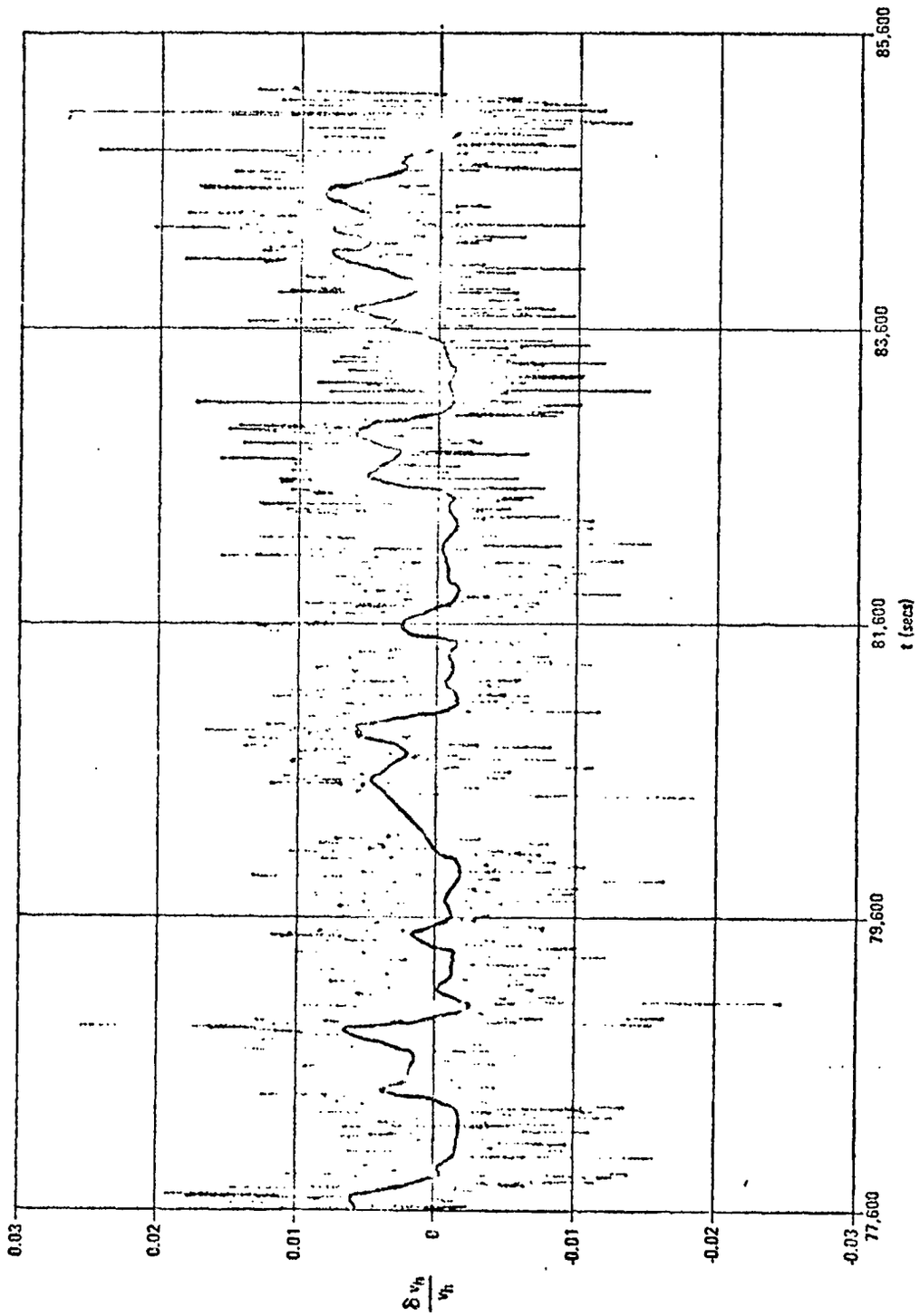

Fig. 4-5 Heading Velocity Error Coefficient

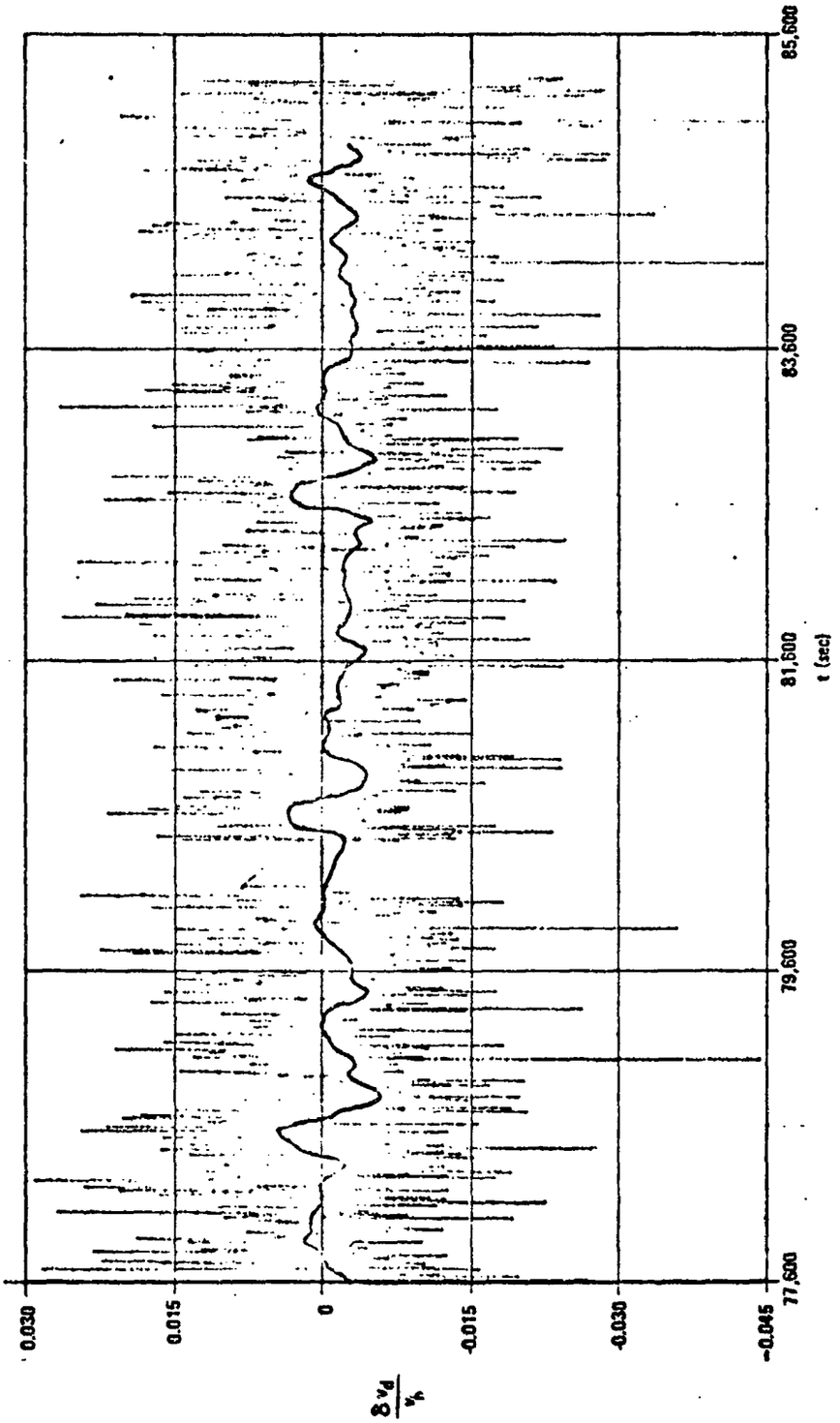

Fig. 4-6 Drift Velocity Error Coefficient

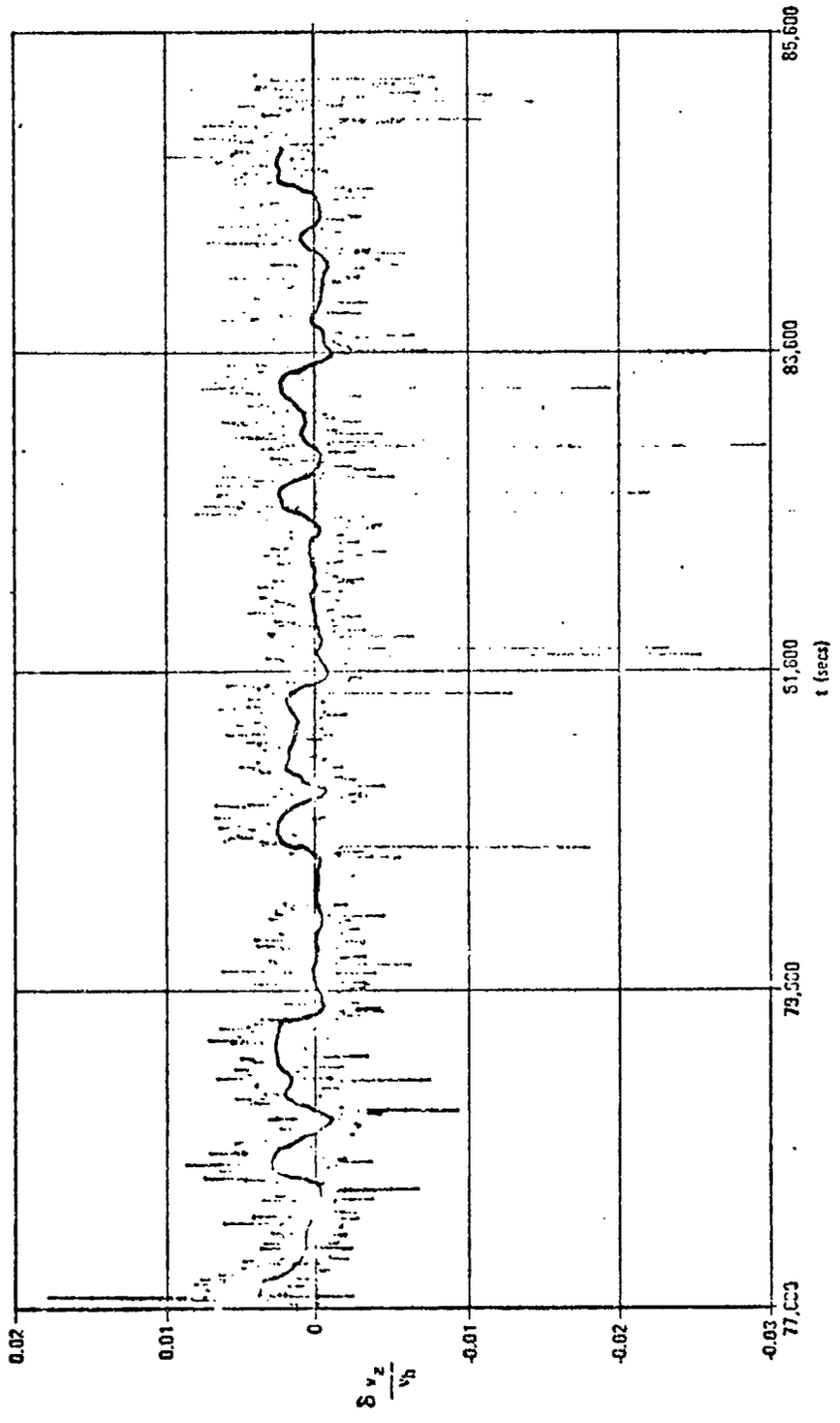

Fig. 4-7 Vertical Velocity Error Coefficient

b) Uncertainty in estimated velocities - the segments should correspond to those portions of the flight where the PFP computed 1 sigma uncertainties in the velocity estimates are low enough so that they do not represent a significant portion of the computed measurement residual, and

c) Significant Sample Size - the selected segments must contain enough samples so that the uncertainty in the computed statistics is much smaller than the actual parameter. Thus, for example, the variance of the sample mean of k samples is given by

$$\sigma_m^2 \leq \frac{\sigma_x^2}{k} \qquad (4\text{-}14)$$

where

σ_m^2 = variance of the sample mean

σ_x^2 = variance of the individual samples

The flight includes 5 straight and level legs, 3 on a southerly heading and 2 to the north, of approximate durations of 8 and 12 minutes respectively. The lack of data points seen in Figs. 4-4 through 4-7 in the 80150-80400 secs interval is due to the presence of a data gap in the Flight Data Tape, so that only about 8 minutes of data are available for the first northerly leg. Interspersed with these legs are 8 left turns and 3 right turns at constant altitude, all at approximately the same 30° bank angle.

From Figs. 4-2 and 4-3, it can be seen that the uncertainties in the estimated velocities are of the order of .06 ft/sec for the horizontal and .11 ft/sec for the vertical, for the straight and level legs, while climbing somewhat at the turns. In either case, however, the values

are well below the level of the doppler induced velocity measurement errors, and are therefore acceptable for data reduction.

At the nominal CAINS readout period of 1 sec, the straight and level segments yield on the order of 400 samples. Also, from Figs. 4-5, 4-6, and 4-7, sample standard deviations of roughly .006, .01 and .003 can be inferred for the doppler residual ratios along each of the aircraft axes. Hence, the following uncertainties in the computed sample means can be expected for this sample size:

$$\sigma_{m_H} = .0003 \quad \text{along heading}$$

$$\sigma_{m_D} = .0005 \quad \text{cross heading (drift)} \qquad (4\text{-}15)$$

$$\sigma_{m_Z} = .00015 \quad \text{along aircraft yaw axis (vertical)}$$

all of which are well below the desired parameter accuracy.

Examination of Figs. 4-5, 4-6, and 4-7 shows significant shifts of the mean at the maneuvering instants. Therefore, it was decided to compute statistics for these portions of the flight, even though the available sample size is significantly smaller than for the straight legs. The average sample size for the turns is on the order of 50 samples, which yields significance levels of

$$\sigma_{m_H} = .00085$$

$$\sigma_{m_D} = .0014 \qquad (4\text{-}16)$$

$$\sigma_{m_Z} = .0004$$

On this basis, then the following segments were selected.

1. Straight and level

t_{start}	t_{stop}	heading	sample size
78950 secs	79400 secs	180°	363
79600 secs	80100 secs	0°	418
81000 secs	81500 secs	180°	420
81700 secs	82490 secs	0°	657
83000 secs	83550 secs	180°	446

2. Left Turns

a) From north heading to south-west heading.

78360 secs	78430 secs	64
80454 secs	80516 secs	58
82507 secs	82589 secs	57

b) From south-west heading to south-east heading

78665 secs	78708 secs	28
80753 secs	80793 secs	28
82780 secs	82823 secs	28

c) From south heading to north heading

79435 secs	79537 secs	78
81520 secs	81620 secs	8[illegible]

3. Right Turns

b) From south-east heading to south heading

78882 secs	78904 secs	21
80950 secs	80975 secs	24
82974 secs	82994 secs	19

After the data reduction process had been completed, it was discovered that the transponder survey data provided to Intermetrics, and used by the PFP, was incorrect. In particular, the assumed survey data for the Stallion transponder (#8), represented a location which is 100 ft above the actual transponder.

The effect of this survey error on the PFP velocity estimates was then investigated. The transponder survey error is exhibited as a discrepancy between the PFP's computed range and the actual CR-100 measured range, with the effect that the estimated aircraft position is displaced to null the difference. The PFP assumes an uncertainty in the measured range due to propagation error, which is proportional to range. Thus, far away from the Stallion transponder, the effect of the survey error is negligible.

On the other hand, around the Stallion transponder overflight, the estimated aircraft state is strongly dependent on measurements to that transponder. It can be shown that for this survey error, the estimated vertical velocity error will exhibit a doublet, centered at the overflight, with a peak value of 1 to 2 ft/sec; and the estimated ahead velocity error will exhibit a triplet, centered at the overflight, with a peak error of approximately 2 ft/sec. This expected behavior is confirmed by Figs. 4-5 and 4-7.

Hence, for an aircraft speed of about 600 ft/sec, the errors in the estimated velocities are of a magnitude larger than the expected Doppler coefficients. Therefore, the data obtained in these regions, i.e., the turns from north heading to southwest heading, and from southwest heading to southeast heading, are not appropriate for recovery of doppler parameters. They are nevertheless included in the following tables for purposes of completeness.

4.4 Statistical Analysis

The following statistical parameters are computed as a measure of the doppler radar errors:

I. Sample Mean, given by

$$m_x = \frac{1}{n} \sum_{i=1}^{n} x_i \tag{4-17}$$

where

n = number of samples

x_i = individual sample at time t_i

II. Standard Deviation, given by

$$\sigma_x = \sqrt{\frac{1}{n-1} \sum_{i=1}^{n} (x_i - m_x)^2} \tag{4-18}$$

III. Cross Correlation Coefficient, given by

$$\rho_{xy} = \left(\frac{1}{n-1} \sum_{i=1}^{n} (x_i - m_x)(y_i - m_y) \right) / \sigma_x \sigma_y \tag{4-19}$$

IV. Auto Correlation Function, given by

$$\phi_{xx}(\tau) = \frac{1}{n} \sum_{i=1}^{n} (x_i - m_x)(x_j - m_x) \tag{4-20}$$

where

$$t_i - t_j = \tau \tag{4-21}$$

for discrete values of τ (0, 1, 2 secs)

Table 4-1 presents sample means and standard deviations computed from the straight and level segments. Sample [illegible] and the significance of the sample mean along each axis also indicated for each segment. Figs. 4-8 and 4-9 present histograms of the sample means for the ahead and drift errors. Table 4-2 presents the cross correlation between the level-axis errors plus the time correlation of each level axis errors.

Table 4-3 presents sample means and standard deivations computed for the turning segments. Figs. 4-10 and 4-11 present histograms of the sample means for the ahead and drift errors for these turning segments.

4.5 Flight Test Results Discussion

4.5.1 Doppler Noise

As expected, the Doppler velocity components contain large additive random error. The one-sigma amplitudes of the random errors, from Table 4-1, were found to be

$$\sigma_{\delta v_h/v_h} = .006$$

$$\sigma_{\delta v_d/v_h} = .010 \qquad (4\text{-}22)$$

$$\sigma_{\delta v_z/v_h} = .003$$

The measured values may be compared with noise specification given in Eq. (3-78). The aircraft velocity in this flight averaged 355 knots. Converting the specifications of Eq. (3-78) to non-dimensional values at 355 knots yield values of .007, .007, and .005. The above measured noises in the heading and drift velocities are seen to be about at the specification level. The measured noise in the vertical velocity is less than the specified level.

Segment	Sample Means			Standard Deviations			Sample Size	Significance of the Sample Mean		
	$\delta v_h/v_h$	$\delta v_d/v_h$	$\delta v_z/v_h$	$\delta v_h/v_h$	$\delta v_d/v_h$	$\delta v_z/v_h$		$\delta v_h/v_h$	$\delta v_d/v_h$	$\delta v_z/v_h$
1. (1^{st} Southerly)	-.0012	-.0014	.0025	.0071	.0115	.0028	363	.00037	.00060	.00015
2. (1^{st} Northerly)	-.0009	-.0007	.0002	.0054	.0094	.0020	418	.00026	.00046	.00010
3. (2^{nd} Southerly)	-.0012	-.0005	.0018	.0087	.0091	.0035	420	.00028	.00044	.00017
4. (2^{nd} Northerly)	-.0008	-.0024	.0002	.0056	.0100	.0025	657	.00022	.00039	.00010
5. (3^{rd} Southerly)	-.0009	-.0003	.0016	.0056	.0093	.0045	446	.00026	.00044	.00021
	Average means			RMS std. deviations						
All five segments	-.0010	-.0011	.0013	.0059	.0099	.0032				

Table 4-1 Sample Means and Standard Deviations for Doppler Error Sources - Straight and Level Segments

INTERMETRICS INCORPORATED • 701 CONCORD AVENUE • CAMBRIDGE, MASSACHUSETTS 02138 • (617) 661-18

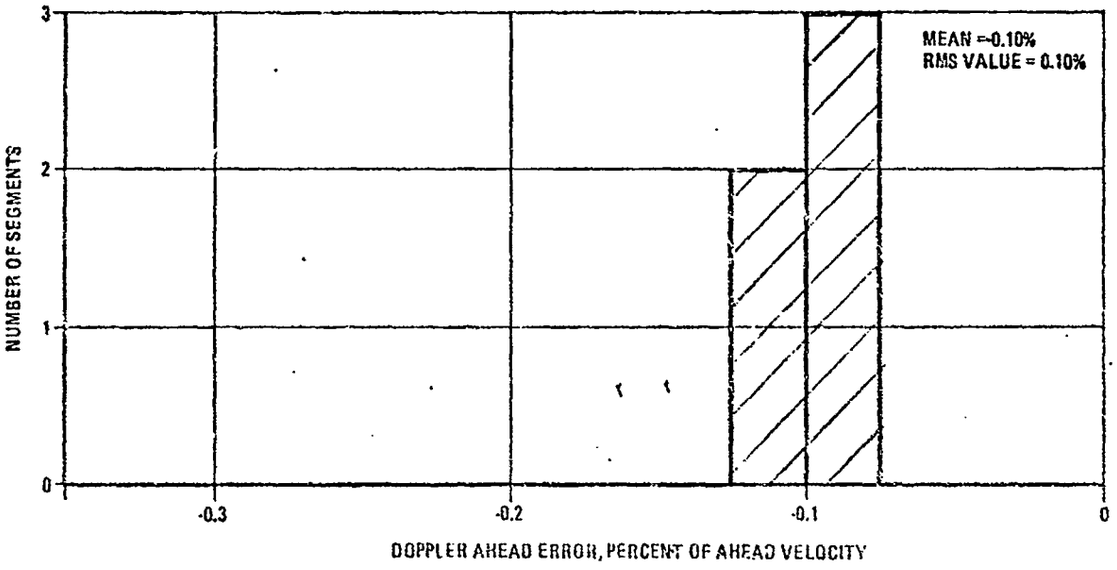

Fig. 4-8 Histogram of Heading Velocity Errors in Level Flight

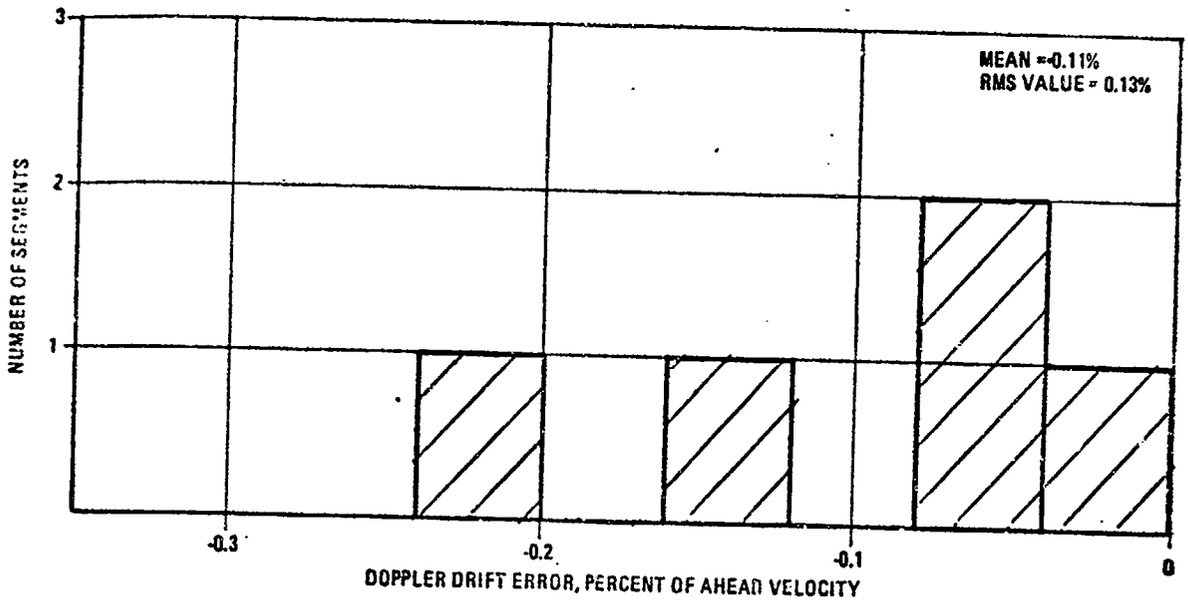

Fig. 4-9 Histogram of Drift Velocity Errors in Level Flight

Segment	Correlation Coefficient ρ_{HD}	Auto Correlations					
		$\phi_{HH}(0)$	$\phi_{HH}(1)$	$\phi_{HH}(2)$	$\phi_{DD}(0)$	$\phi_{DD}(1)$	$\phi_{DD}(2)$
1	.06	5.0×10^{-5}	1.7×10^{-5}	9.9×10^{-6}	1.3×10^{-4}	4.2×10^{-5}	1.8×10^{-5}
2	-.06	2.9×10^{-5}	2.3×10^{-6}	2.7×10^{-6}	8.8×10^{-5}	5.1×10^{-7}	3.1×10^{-6}
3	-.04	3.2×10^{-5}	-2.1×10^{-6}	-1.6×10^{-6}	8.3×10^{-5}	-6.3×10^{-7}	-2.5×10^{-6}
4	-.08	3.1×10^{-5}	1.3×10^{-6}	-2.4×10^{-6}	1.0×10^{-4}	5.4×10^{-6}	-9.6×10^{-7}
5	-.04	3.1×10^{-5}	-9.0×10^{-7}	-1.9×10^{-6}	8.6×10^{-5}	-4.0×10^{-7}	-4.3×10^{-6}

Table 4-2 Correlations for Doppler Errors - Straight and Level Segments

ITHACO, INCORPORATED • 701 CONCORD AVENUE • CAMBRIDGE, MASSACHUSETTS 02138 • (617) 661-1840

Segment	Sample Means			Standard Deviations			Sample Size	Significance of the Sample Mean		
Left Turns:	$\delta v_h/v_h$	$\delta v_d/v_h$	$\delta v_z/v_h$	$\delta v_h/v_h$	$\delta v_d/v_h$	$\delta v_z/v_h$		$\delta v_h/v_h$	$\delta v_d/v_h$	$\delta v_z/v_h$
From North heading to Southwest heading*										
1	.0053	-.0028	0.	.0070	.0098	.0031	64	.00088	.0012	.00039
2	.0051	-.0046	-.0012	.0052	.0115	.0034	58	.00068	.0015	.00045
3	.0061	-.0045	.0007	.0076	.0107	.0029	57	.0010	.0014	.00038
From Southwest heading to Southeast heading*										
1	-.0006	-.0048	-.0015	.0056	.0110	.0023	28	.0010	.0021	.00044
2	.0002	-.0046	0.	.0051	.0099	.0027	28	.00096	.0019	.00051
3	.0017	-.0016	.0018	.0052	.0079	.0045	28	.00098	.0015	.00085
From South heading to North heading										
1	.0030	-.0059	-.0012	.0063	.0109	.0024	78	.00071	.0012	.00027
2	.0043	-.0023	-.0009	.0064	.0096	.0022	80	.00071	.0011	.00025
Right Turns:										
From Southeast heading to South heading										
1	.0014	-.0047	.0028	.0080	.0066	.0019	21	.0017	.0014	.00041
2	.0031	-.0030	.0027	.0054	.0107	.0020	24	.0011	.0022	.00041
3	.0019	-.0019	.0006	.0048	.0094	.0083	19	.0011	.0021	.0019

*These segments are corrupted by transponder 8 survey error

Table 4-3 Sample Means and Standard Deviations for Doppler Error Sources - Turning Segments

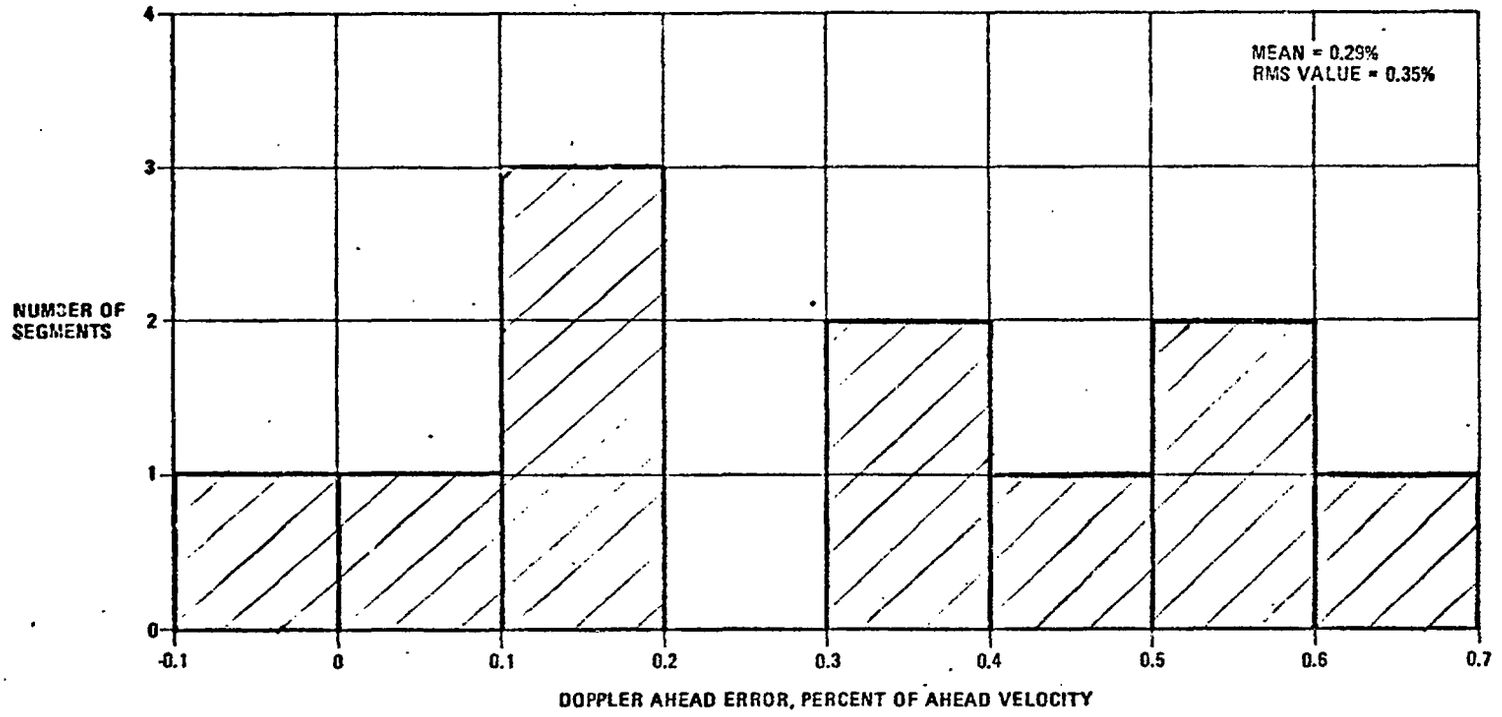

Fig. 4-10 Histograms of Heading Velocity Errors in Turning Flight

TERMETRICS INCORPORATED • 701 CONCORD AVENUE • CAMBRIDGE, MASSACHUSETTS 02138 • (617) 661-1840

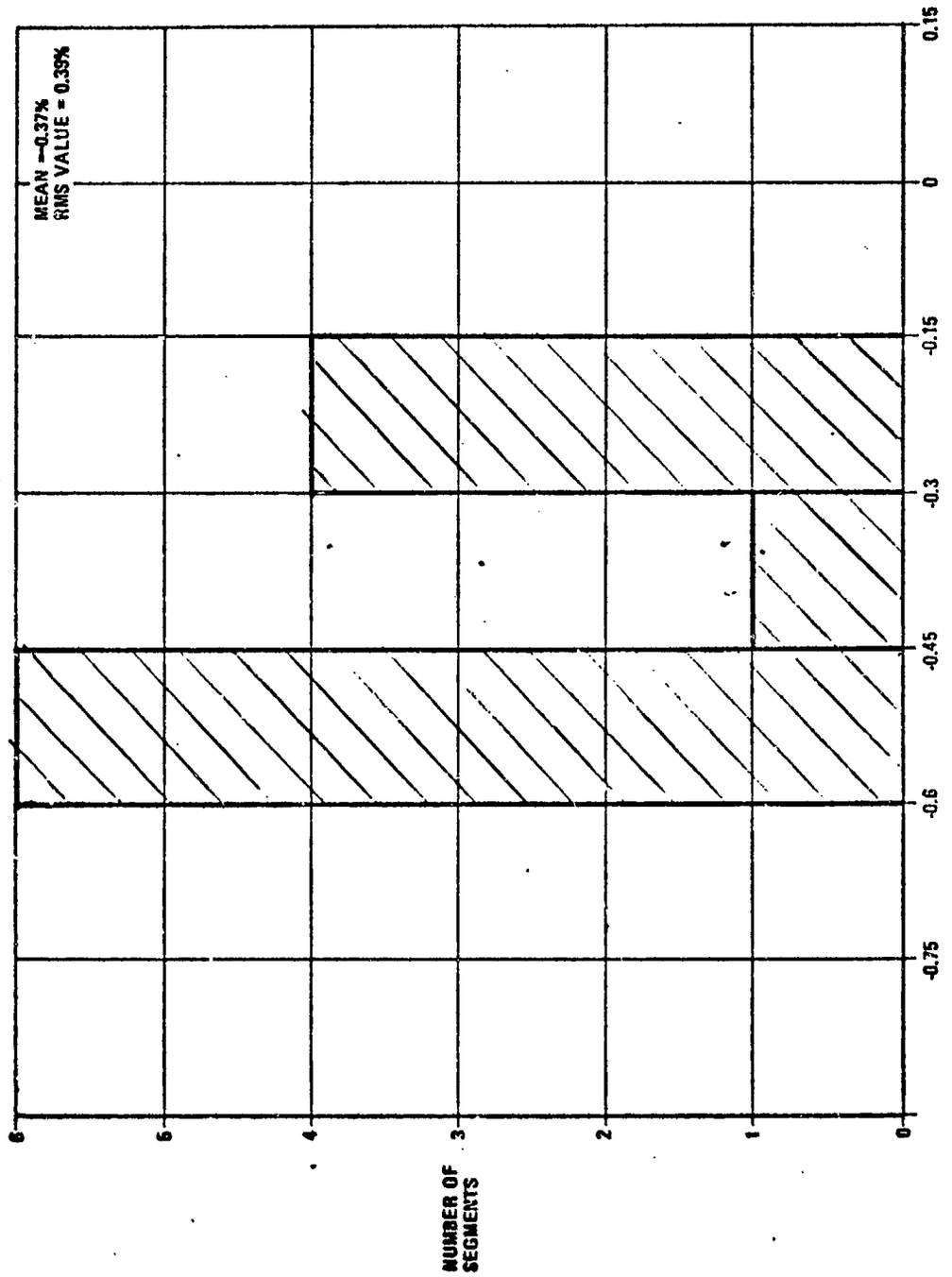

Fig. 4-11 Histogram of Drift Velocity in Turning Flight

In theory, the cross-correlation between the components of Doppler velocity random error should be zero. As discussed in Section 3.2.3, this can be shown assuming independent random error in each beam velocity and by taking into account the four-beam-array symmetry. The measured correlation coefficient between the heading velocity random error and the drift velocity random error was shown in Table 4-2. It is seen to be small, in agreement with theory.

In theory the Doppler velocity random error should have a very short correlation time, of the order of the 0.2 sec Doppler output time constant. The measured autocorrelations of the heading and drift components of the Doppler error were presented in Table 4-2. The values of correlation at $\tau = 1$ and $\tau = 2$ sec are seen to be generally an order of magnitude below the values at $\tau = 0$. These results are consistent with the correlation time being less than one sec.

4.5.2 Slowly Varying Errors in Level Flight

During the five segments of straight and level flight, the ahead velocity error variable was found to have segment mean values ranging from -.0008 to -.0012 (Table 4-1). The average value for all segments was -.0010. According to the Doppler error model summarized in Section 3.10 and in particular according to the expected one-sigma values for elements of the velocity error matrix (Eq. 3-80), for small drift and vertical velocity the ahead error is expected to be about .0014. The measured ahead error is found to be slightly smaller than expected.

The drift velocity error (Table 4-1) was found to vary from -.0003 to -.0024. The average value for all five segments was -.0011. According to the Doppler error model summarized in Section 3.10, the non-dimensional drift error variable is dominated by the contributions of the two velocity error matrix elements E_{dh} and E_{dd}

$$\delta v_d / v_h = E_{dh} + E_{dd}\, v_d / v_h \qquad (4\text{-}23)$$

These elements according to Eq. (3-80) are expected to have one-sigma values of .00067 and .00823, respectively. During the northerly and southerly legs of the flight there was a crosswind of about 60 ft/sec, which produced an equal magnitude drift velocity whose sign depended on the flight direction (north or south). The heading velocity was 600 ft/sec. For the drift to heading velocity ratio of 0.1, the second term in Eq. (4-23) is expected to have one-sigma value of .00082. The combination of the two terms having one sigma values of .00067 and .00082 with the sign of the larger term alternating with flight direction would produce a drift velocity error having large shifts in value with flight direction. This characteristic is indeed observed in the measured drift velocity error in Table 4-1. The data is biased (mean value -.0011) more than is expected considering the one sigma value of E_{dh} of .00067. Some contributor to Edh is larger than expected. Perhaps the Doppler-with-respect-to-INS installation azimuth alignment is larger than the assumed .0006 radians (2 arc min).

The vertical velocity error (Table 4-1) was found to vary from .0002 to .0025. The average value for all five segments was .0013. According to the Doppler error model summarized in Section 3.10, for normally small drift and vertical velocities, the vertical velocity error should be dominated by the element E_{zh} which is expected to have one-sigma value of .00303. The measured vertical velocity error is below the expected one sigma value, indicating that the velocity error matrix element E_{zh} may be smaller than expected. The largest contributor to E_{zh} was assumed to be the Doppler-with-respect-to-INS installation pitch alignment error of 10 arc min one sigma. Note that the measured vertical velocity error shifts significantly with heading. Such behavior could be caused by a steady INS readout error caused by steady platform tip about east of the order of .0008 radian (3 arc min). Such a large steady tip could be caused by an 800 μg north accelerometer bias or a 3 arc min north accelerometer misalignment about the platform east axis.

4.5.3 Slowly Varying Errors in Maneuvering Flight

As indicated in Section 4.3, significant shifts in the mean velocity errors are observed during the turns. Therefore separate sample means were computed for these

segments and were presented in Table 4-3. The tabulated results show component velocity errors several times larger than those for level flight.

As mentioned earlier, the sets of data near transponder 8 should be disregarded, because an error in the assumed altitude of the transponder (survey data) produced significant velocity error in the best-estimate-of velocity as obtained by the CIRIS Post Flight Processor (PFP).

An additional source of reference error was discovered, but found to be negligible. A wrong value was used in the PFP for the CR-100 ranging system antenna lever arm. The given roll axis component was too large by the order of 4 ft. Based on similar considerations as for the Doppler antenna lever arm, this effect does not contribute more than 0.1 ft/sec and hence is negligible.

Several Doppler-velocity-measurement sources of error are expected to have varying and perhaps larger values during maneuvers. Some of these in the velocity error matrix are the lateral terrain bias, the INS attitude read-out (resolver) error, and the INS-Doppler installation alignment (if there is a significant maneuver g level). In addition the effect of velocity lag due to Doppler time constant can become significant.

However, it is also true that the reference system velocity errors may also be larger during maneuvers. The CIRIS reference system, at the time of this 7 August 1973 flight, was just reaching operational status. As with any new system, it is likely that a few bugs were not yet discovered and corrected. The transponder 8 survey error is one error that has subsequently been discovered and corrected. The indicated velocity from the CAINS inertial system had shifts in apparent velocity error during turns as if there were horizontal accelerometer scale factor errors of ASF_x = 4000 ppm and ASF_y = -4900 ppm. This observed systematic error in the INS velocity was compensated in the Post Flight Processor, as indicated by Eq. (4-7). However, we cannot be certain that this error (whatever its source) has been entirely eliminated. Therefore the possibility

exists that the CIRIS PFP indicated velocity is not as accurate as the PFP-computed uncertainties presented in Fig. 4-2 and 4-3.

Accordingly we hesitate to conclude that the measured velocity differences for maneuvering flight are due to degraded Doppler performance during these maneuvers.

CHAPTER 5

SUMMARY AND CONCLUSIONS

A Teledyne-Ryan APN-200 Doppler velocity sensor has been added to the Holloman Air Force Base CIRIS (Completely Integrated Reference Instrumentation System). The major CIRIS sensors include a Litton LAINS inertial navigator with barometric altimeter, a Cubic Corp. CR-100 precision ranging system, and now the APN-200 Doppler. Intermetrics was asked to modify the CIRIS Post-Flight Processor to incorporate the Doppler measurements into the optimal estimation of the aircraft navigation state (position, velocity, attitude). This requires an error model representing the sources of error in the APN-200 Doppler velocity sensor. This report provides such an error model. Also flight test data have been analyzed to confirm the statistical parameters in the error model.

A brief discussion of Doppler sensor principles is presented, as well as a discussion of the specific functional design of the APN-200. This introduction makes the report self contained, by providing the necessary background for the discussion of the individual sources of error. Performance limits that are implied by the functional design are discussed.

The individual sources of error in a Doppler velocity measurement were discussed, including estimates of their one-sigma values. Many of the sources of error are a function of the design of the Doppler velocity sensor. In addition, several external environment factors are sources of error. Also included in the error discussion is the velocity error due to attitude reference error.

Doppler velocity error is shown to contain a large amplitude random error in all three components. However, because of its short correlation time, after processing many

Doppler measurements the effect of this zero-mean random error is reduced to a negligible level.

The more significant Doppler errors are the lower level constant or slowly varying errors. Many of the constant or slowly varying sources of error contribute to velocity error as elements of a 3 by 3 velocity-error matrix (velocity error being the product of this matrix times the velocity vector). For the assumed one-sigma values of the APN-200 and other sources of error, and assuming moderate or small values of lateral (drift) velocity and vertical velocity, the most significant elements of this matrix are E_{hh}, E_{dh}, E_{dd}, and E_{zh}.

E_{hh} is the element relating ahead velocity error to ahead velocity (scale factor error). The largest contributor to this element is estimated to be the Doppler beam direction error due to the antenna being at a temperature different from that at which it was calibrated.

E_{dh} is the element relating drift velocity error to ahead velocity (azimuth alignment error). The largest contributor to this element is estimated to be the alignment error between the INS inside the aircraft and the Doppler antenna mounted on the outside of the aircraft.

E_{dd} is the element relating drift velocity error to drift velocity (lateral scale factor error). The largest contributor to to this element is estimated to be the terrain bias effect over the smooth barren terrain of the Tularosa Basis in New Mexico. Over smooth water the terrain bias effect would be larger. Over rough or wooded terrain the effect would be less.

E_{zh} is the element relating vertical velocity error to ahead velocity (pitch alignment error). The largest contributor to this element is estimated to be the alignment error between the INS and the Doppler antenna.

A brief discussion was presented on how the complete error model may be simplified for the purpose of Kalman filter synthesis. Three state variables may be used to represent the Doppler velocity measurement slowly varying error in each velocity component.

The data from a flight test of the APN-200 were analyzed. The Doppler measured velocity was compared with an estimate of vehicle velocity provided by the optimal combination of the CIRIS inertial and precision ranging data. The optimal processor has a self-estimate that its velocity errors were less than 0.1 ft/sec for east and north velocity components and less than 0.2 ft/sec for the vertical velocity component. However at this early stage in the debugging of the CIRIS system, it is possible that unmodeled sources of error (in the inertial system, in the precision ranging system, in the flight software, or in the optimal Post Flight Processor) may have caused reference velocity errors larger than the above values. Thus the computed differences between the measured APN-200 Doppler velocity and the estimated reference velocity may be an indication not only of the Doppler errors but also the reference errors. All that can be concluded with certainty is that the Doppler errors must be less than or equal to the observed differences.

The analysis of the velocity differences showed the large amplitude random error to be at the specification level in the ahead and lateral components and to be less than the specification level in the vertical component.

The constant or slowly varying portions of the velocity differences in level flight were at the expected level for Doppler forward velocity error and for Doppler lateral velocity error. The vertical velocity difference was somewhat smaller than the expected one-sigma value for Doppler vertical velocity error.

In maneuvering flight, the observed slowly-varying portions of the velocity differences were several times larger than the corresponding errors in level flight. Several sources of error are known to provide increased Doppler velocity error during maneuvers. However, the reference velocity may also have had increased velocity error during the maneuvers. Therefore no firm conclusions can be drawn from this limited data with respect to the APN-200 error characteristics during maneuvers.

Previous flight tests of Doppler velocity sensors have generally performed a time integration of the Doppler velocity measurements and compared the indicated position with a reference position. The flight test data reduction in this report has directly compared the Doppler velocity outputs with a precision velocity reference trajectory. This approach permits examination of the Doppler random error as well as examination of the slowly varying error as a function of flight conditions, such as heading, cross-wind, and attitude. This approach has the greatest promise of exposing the individual sources of error that are making the largest contribution to Doppler velocity error.

REFERENCES

1. Anon., "Proposal: AN/APN-200 Doppler Velocity Sensor for Long Range Patrol Aircraft", TRA 29070-179, Teledyne Ryan, San Diego, Cal., January 1973.

2. Fried, Walter R., "Doppler Navigation", Chapter 6 of Avionic Navigation Systems, M. Kayton and W. R. Fried, editors, John Wiley & Sons, New York 1969.

3. VanderStoep, D.R., Call, R.W., and Warzynski, R.R., "A New Approach to Doppler-Inertial Navigation (Doppler Beam Sampling)", presented at the 6th Asilomar Conference on Circuits and Systems, Monterey, California, 15-17 November 1972.

4. Berger, F.B., "The Nature of Doppler Velocity Measurement", IRE Transactions on Aeronautical and Navigational Electronics, Vol. 4, September 1957, pp. 103-112.

5. Widnall, W. S., Carlson, N.A., Grundy, P.A., "Post-Flight Processor for CIRIS", TR 16-72, Intermetrics, Cambridge, Mass., 24 November 1972.

6. Pitman, G.R., editor, et al, Inertial Guidance, John Wiley and Sons, New York, 1962.

7. Britting, K.R., Inertial Navigation System Analysis, Wiley-Interscience, 1971.

8. Widnall, W.S., and Grundy, P.A., "Inertial Navigation System Error Models", TR 03-73, Intermetrics, Cambridge, Mass., 11 May 1973.